THE JOURNAL OF PHYSICAL CHEMISTRY B

Article

pubs.acs.org/JPCB

Liquid–Liquid Extraction of Uranyl by an Amide Ligand: Interfacial Features Studied by MD and PMF Simulations

G. Benay and G. Wipff*

Laboratoire MSM, UMR 7177, Institut de Chimie, 1 rue B. Pascal, 67000 Strasbourg, France

Supporting Information

ABSTRACT: We report a molecular dynamics study of biphasic systems involved in the liquid–liquid extraction of uranyl nitrate by a monoamide ligand (L = *N,N*-di(2-ethylhexyl)isobutyramide, DEHiBA) to hexane, from pH neutral or acidic (3 M nitric acid) aqueous solutions. We first describe the neat interfaces simulated with three electrostatic models, one of which including atomic polarizabilities. The free energy profiles for crossing the water/hexane interface by L or its $UO_2(NO_3)_2L_2$ complex are then investigated by PMF (potential of mean force) calculations. They indicate that the free ligand and its complex are surface active. With the polarizable force field, however, the complexes have a lower affinity for the interface than without polarization. When DEHiBA gets more concentrated and in acidic conditions, their surface activity diminishes. Surface activity of $UO_2(NO_3)_2L_2$ complexes is further demonstrated by demixing simulations of randomly mixed DEHiBA, hexane, and neutral or acidic water. Furthermore, demixing of randomly mixed solvents, L molecules, $UO_2(NO_3)_2$ salts, and nitric acid shows in some cases complexation of L to form $UO_2(NO_3)_2L_2$ and $UO_2(NO_3)_2L$ complexes that adsorb at the aqueous interfaces. These features suggest that uranyl complexation by amide ligands occurs "right at the interface", displaying marked analogies with the liquid–liquid extraction of uranyl by TBP (tri-*n*-butyl phosphate). Regarding the positive effect of nitric acid on extraction, the simulations point to several facets involving enhanced ion pairing of uranyl nitrate, decreased affinity of the complex for the interface, and finally, stabilization of the complex in the organic phase.

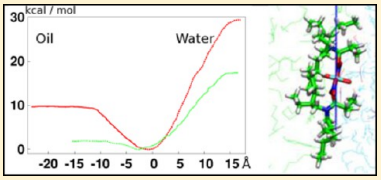

INTRODUCTION

Ion separation by liquid–liquid extraction is the cornerstone of nuclear waste separation and partitioning.[1−3] A major step in the industrial PUREX process is the separation of $U^{(VI)}$ and $Pu^{(IV)}$ from aqueous solutions obtained by dissolution of irradiated fuel in nitric acid, using TBP (tri-*n*-butyl-phosphate) as extractant molecule. Using TBP has, however, some drawbacks, like formation of degradation products (alkyl phosphates) that can cause the deleterious formation of third phase and/or precipitation. Furthermore, TBP contains phosphorus that can hardly be decomposed to gases by incineration and vitrification of the extracted complexes. Thus, alternative strategies, using other extracting agents deserve research developments. Among the many synthesized ligands, *N,N*-dialkylamides (monoamides RC(O)NR′$_2$; Scheme 1) display promising features: they are soluble in commercially available hydrophobic solvents, they are fully incinerable ("CHON principle"[4]), they are as stable as TBP toward radiolysis in the presence of nitric acid, and they afford degradation products that do not seem to have detrimental effects on extraction properties.[5−9] Like TBP, they extract uranyl as neutral complex of $UO_2(NO_3)_2(ligand)_2$ composition,[10] where the U atom is hexacoordinated in the equatorial plane. Different linear or branched R and R′ alkyl substituents have been compared (see, e.g., structure–activity relationship studies[11−13]), showing that DEHiBA (*N,N*-di(2-ethylhexyl)-isobutyramide, also hereafter noted in short as "L" ligand; see Scheme 1) has the potential impact to extract $U^{(VI)}$ selectively from acidic aqueous solutions of irradiated nuclear fuel.[14,15]

Beyond the coordination chemistry of the extracted metal, the solution behavior of the different partners can be crucial for understanding and further improving the liquid–liquid extraction processes. Important issues concern the nature of the heterogeneous mixed solutions, and how the extractant meets and "recognizes" the extracted ion, i.e., "what happens at the liquid–liquid interface" between the source and receiving phases, with related mechanistic and kinetic issues.[16−19] Important insights into the interfacial landscape emerge on the experimental side from surface tension and surface spectroscopy studies, as recently reported for DEHiBA.[20,21] See also diffraction studies on water/oil mixtures with extractant molecules like TBP or diamides.[22,23] These support mental representations based on physical

Scheme 1. Monoamides

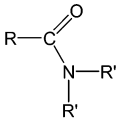

DEHiBA: R = $CH(CH_3)_2$
R' = $CH_2CH(C_2H_5)C_4H_9$
DMAA: R = R' = CH_3
DMtBA: R = ^{t}Bu, R' = CH_3

Received: March 22, 2013
Revised: May 22, 2013

   dx.doi.org/10.1021/jp4028386 | *J. Phys. Chem. B* XXXX, XXX, XXX–XXX

Table 1. Systems Studied by MD (Juxtaposed Liquids), PMF, and Mixing–Demixing Simulations, with L = DEHiBA

	solute (s)	N_{Hex}	water	box size $x^*y^*(z_{oil} + z_{wat})$ (Å^3)	time (ns)
juxtaposed liquids		301	2119 H_2O	40 × 40 × (39 + 41)	5/0/0[b]
		301	20 "acid"[a]	37 × 37 × (44 + 32)	5/0/5[b]
	8 L[c]	217	2091 H_2O	38 × 38 × (33 + 44)	5/0/5[b]
	8 L[c]	221	20 "acid"[a]	36 × 36 × (38 + 35)	5/0/5[b]
	60 L[d]	149	2113 H_2O	35 × 35 × (51 + 55)	5/5/5[b]
	60 L[e]	150	20 "acid"[a]	34 × 34 × (61 + 40)	5/5/5[b]
	40 L + 20 LH^+[f]	246	20 "acid"[a]	35 × 35 × (65 + 41)	5/0/0[b]
mixing–demixing	60 L[e]	150	20 "acid"[a]	34 × 34 × 101	10/25/5[b]
	5 $UO_2(NO_3)_2$ + 50 L	42	2012 H_2O	36 × 36 × 77	5/15/5[b]
	5 $UO_2(NO_3)_2$ + 50 L	39	205 H_2O	34 × 34 × 42	5/15/5[b]
	5 $UO_2(NO_3)_2$ + 50 L	45	19 "acid"[a]	34 × 34 × 72	5/10/5[b]
	5 $UO_2(NO_3)_2$ + 50 L	58	5 "acid"[a]	35 × 35 × 45	5/15/5[b]
	5 $UO_2(NO_3)_2(L)_2$ + 40 L	60	2115 H_2O	37 × 37 × 79	5/0/5[b]
	5 $UO_2(NO_3)_2(L)_2$ + 40 L	64	20 "acid"[a]	35 × 35 × 74	5/0/5[b]
PMF	1 L[g]	298	2086 H_2O	40 × 40 × (39 + 41)	1[h]
	1 L[g]	298	20 "acid"[b]	38 × 38 × (39 + 36)	5[h]
	1 + 59 L[d]	149	2113 H_2O	35 × 35 × (51 + 55)	2[h]
	1 + 59 L[e]	150	20 "acid"[b]	34 × 34 × (61 + 40)	2[h]
	1$UO_2(NO_3)_2(L)_2$	292	2052 H_2O	40 × 40 × (39 + 40)	1[h]
	1 $(L)_2UO_2$ $(NO_3)_2$	288	20 "acid"[b]	37 × 37 × (38 + 37)	1[h]
	1 + 4 $UO_2(NO_3)_2(L)_2$ + 40 L	60	2115 H_2O	37 × 37 × (34 + 45)	1[h]
	1 + 4 $UO_2(NO_3)_2(L)_2$ + 40 L	64	20 "acid"[b]	35 × 35 × (35 + 39)	1[h]
	1 $Eu(NO_3)_3(L)_3$	288	2073 H_2O	40 × 40 × (39 + 40)	1[h]
	1 $Eu(NO_3)_3(L)_3$	288	20 "acid"[b]	37 × 37 × (38 + 37)	1[h]
	8 L[i]	221	20 "acid"[a]	36 × 36 × (38 + 35)	5[h]
	60 L[i]	150	20 "acid"[a]	34 × 34 × (61 + 40)	5[h]

[a]"acid": 3 NO_3^- + 3 H_3O^+ + 1 HNO_3 + 62 H_2O to obtain 3 M nitric acid with 75% dissociation. [b]Simulations with STD/SCAL/POL models. [c][L] ≈ 0.3 M in hexane. [d][L] ≈ 1.6 M in hexane. [e][L] ≈ 1.4 M in hexane. [f][L + LH^+] ≈ 1.2 M in hexane [g][L] ≈ 0.03 M in hexane. [h]MD equilibration before starting the PMF for 60 ns. STD model. [i]PMF for a HNO_3 molecule.

models, without providing detailed views of the solutions and interfaces. Such features can be obtained in principle by molecular dynamics (MD) simulations, based on all-atom representations of the heterogeneous nanosolutions. See, for instance, the cases of TBP[24−26] and of ion extraction by macrocyclic ligands (crown ethers, cryptands, calixarenes).[27−30] We thus decided to study biphasic systems involved in the uranyl extraction by DEHiBA: the interface, neat, and in the presence of uranyl nitrate ions, comparing pH neutral to nitric acid solutions (about 3 M concentration in this study) like in nuclear waste solutions obtained by dissolution of irradiated fuel in nitric acid. We want to see how the complexing groups (amide carbonyl) are oriented at the interface and in the bulk oil phase. What is the nature of the oil phase: is it homogeneous? How much water and acid are extracted? A major issue for the ion extraction process is the interface crossing by the extracted complex: does it correspond to an energy barrier or to an energy trap, as in the case of the uranyl extraction by TBP? What is the effect of nitric acid?

In this paper, we first describe neat biphasic systems (without uranyl nitrate), based on MD simulations on juxtaposed liquids, to characterize the oil phase and the interface, in acidic and neutral conditions, at different DEHiBA concentrations. Because these neat systems have been recently studied by surface tension measurements and surface spectroscopy,[20,21] we analyze the extraction of water and acid and the characteristics of the interface. Then, following previous MD studies on uranyl extraction by TBP,[25] we explore the energetics of the interface crossing by the most relevant species (the free ligand, its neutral complex $UO_2(NO_3)_2(DEHiBA)_2$), by calculating the corresponding free energy profiles, in different conditions. Since trivalent lanthanides are not extracted by amide ligands,[8,31] we also present the free energy profiles for interface crossing by the $Eu(NO_3)_3(DEHiBA)_3$ analogue of the uranyl complex to compare their interfacial behavior. Finally, as also reported for TBP,[24,28,32] we performed mixing–demixing experiments of "randomly" mixed water, hexane + DEHiBA, uranyl nitrate, in neutral and acidic conditions, to test whether the amide ligands will spontaneously complex uranyl nitrate and what is the partitioning of the complex formed, if any. On the methodological side, we compare three force field representations of the systems (neat interfaces and mixing–demixing simulations with uranyl nitrate): the STD and SCAL models based on pairwise 1−6−12 additive potentials, differ by the DEHiBA polarity, while the POL model includes explicit polarization on all atoms (vide infra).

METHODS

MD Simulations of Biphasic Solutions. Molecular dynamics simulations were performed with the AMBER10 software[33] with the following representation of the potential energy U:

dx.doi.org/10.1021/jp4028386 | J. Phys. Chem. B XXXX, XXX, XXX−XXX

$$U = \sum_{\text{bonds}} k_i(l - l_0)^2 + \sum_{\text{angles}} k_\theta(\theta - \theta_0)^2 + \sum_{\text{dihedrals}} \sum_{n} V_n(1 + \cos(n\varphi - \gamma)) + \sum_{i<j} \left[\frac{q_i q_j}{R_{ij}} - 2\varepsilon_{ij}\left(\frac{R^*_{ij}}{R_{ij}}\right)^6 + \varepsilon_{ij}\left(\frac{R^*_{ij}}{R_{ij}}\right)^{12} \right]$$

It accounts for the deformation of bonds, angles, dihedral angles, and electrostatic and van der Waals interactions (assumed to be pairwise additive in this 1−6−12 potential). The solvents were represented explicitly at the molecular level, using the TIP3P model for water[34] and OPLS united atom model for hexane.[35] The UO_2^{2+} Lennard-Jones parameters and charges were fitted on its free energy of hydration.[36] Note that q_U and q_O charges (2.50 and −0.25 e, respectively) are identical to those recently developed by Rai et al.[37] Charges on DEHiBA were fitted on electrostatic potential obtained by QM calculations (DFT/B3LYP/6-31G* level). These ESP charges are given in Table S1 in the Supporting Information. The corresponding force field model, used in conjunction with TIP3P water and the above parameters for acid and uranyl nitrate, will be referred to as standard "STD" model. The ESP charge of the carbonyl oxygen (q_O = −0. 533 e) is low, however, compared to the $q_{O(H2O)}$ charge of −0.834 e, thereby possibly underestimating interactions of DEHiBA with uranyl or H-bond donors. We thus decided to test a set of more polar DEHiBA charges (SCAL model), obtained by scaling the ESP charges of DEHiBA by a factor 1.5, yielding $q_{O(carbonyl)}$ = −0.800. This charge is close to the O_{TBP} charge (from −0.81 to −0.87 e, depending on the model)[26] used in previous work to simulate the TBP analogue of DEHiBA. An alternative approach was to simulate the systems with the ESP charges on DEHiBA, in conjunction with explicit account of polarization effects on all atoms,[38] as represented in AMBER.[33] In that case (referred to here as "POL" calculations), we used the POL3 model for water[39] and the atomic polarizabilities of other atoms listed in Table S1. Interactions energies between $UO_2(NO_3)_2$ or UO_2^{2+} and DEHiBA, as well as H-bonding interactions between DEHiBA and H_2O or HNO_3, calculated with the three electrostatic models are reported in Tables S2 and S3 in the Supporting Information, and compared with QM results obtained with the DMAA (*N*,*N*-dimethylacetamide) and the DMtBA (*N*,*N*-dimethyl-*tert*-butylamide) mimics of DEHiBA (see Scheme 1 and Table S4 in the Supporting Information). Uranyl and europium complexes were simulated as preformed entities, with weak harmonic constraints on $U\cdots O_{AMID}$, $U\cdots O_{NO3}$ "bonds" (at 2.49 and 2.46 Å, respectively) and on $Eu\cdots O_{AMID}$ and $Eu\cdots O_{NO3}$ "bonds" (at 2.49 and 2.47 Å, respectively, with force constants of 20 kcal/mol/Å^2) to avoid dissociation and to retain a bidentate coordination of nitrates during the dynamics. Nitric acid was represented by a 25:75 mixture of HNO_3 and $H_3O^+NO_3^-$ species in water, with the same parameters as in ref 32. Nonbonded interactions were calculated with a 12 Å atom based cutoff, correcting for the long-range electrostatics by using the Ewald summation method (PME approximation).[40] All biphasic solutions were simulated with 3D-periodic boundary conditions, thus as alternating slabs of water and "oil" in the case of juxtaposed solvent liquids. Their characteristics are given in Table 1.

Preparation of the Solutions. We started from adjacent boxes of water and oil with an *xy* section of 40 Å length each, and *z*-length ranging from 10 to 80 Å, depending on the oil:water volumic ratio, and the size and concentration of the solute. The latter was immersed where it is in principle soluble, i.e., DEHiBA and its complexes in the hexane phase, acid or uncomplexed uranyl or europium salts in water. All systems were first relaxed by 3000 steps of energy minimization and by a MD simulation of 0.5 ns at 300 K and a constant pressure of 1 atm to adjust the densities. As a consequence, the relaxed box sizes and exact concentrations of the solutes somewhat differ from one system to the other (Table 1). Subsequent dynamics were performed at constant volume. The temperature was maintained (unless otherwise specified) at 300 K by coupling the solution to a thermal bath using the Berendsen algorithm[41] with a relaxation time of 0.2 ps. The MD trajectories and velocities were calculated using the Verlet algorithm with a time step of 2 fs, in conjunction with SHAKE holonomic constraints on O−H, C−H, and N−H bonds.

Mixing−Demixing Simulations. We first equilibrated biphasic solutions for 0.5 ns at constant pressure (P = 1 atm) to adjust the densities of the two phases, followed by at least 1 ns at constant volume. Mixing was then achieved by a MD run of 1 ns at a temperature of 500 K, with Coulombic interactions divided by a factor 1000 to afford "random" distributions. This was followed by demixing simulations of at least 5 ns with reset electrostatics at a temperature of 300 K.

Analysis of the Trajectories. The trajectories were saved and analyzed every picosecond. Solvent and solute densities were calculated as a function of the *z*-coordinate (perpendicular to the interface) in slices of Δz = 0.2 Å width, and the position of the "interface" (z = 0; Gibbs dividing surface) was dynamically defined by the intersection of the hexane and water (or water + acid, when present) density curves. The densities of solvents and solutes, averaged over the last 1 ns, were plotted as a function of their *z*-position. Interaction energies ΔE_{int} between the solute and solvent(s) were calculated with a 12 Å cutoff and PME correction, with either STD or SCAL models that are based on pairwise additive nonbonded interactions. The orientation of carbonyl groups with respect to the interface was defined by the order parameter $S(z) = \langle(3\cos^2\theta - 1)/2\rangle$, where θ is the angle between the C═O and *z*-axis (perpendicular to the interface). $S(z)$ was averaged in Δz slices of 0.5 Å.

The interfacial surface S_{itf} was calculated at each saved configuration as follows: the *xy* area is divided as a grid of $\Delta x \cdot \Delta y$ elements of $z > 0$ (water side) and $z < 0$ (oil side). For each of them, one calculates the *z*-itf position, equidistant from the *z*-min-H_2O position of H_2O molecules that retain contacts with the aqueous phase, and from the *z*-max-oil position of oil molecules that retain contacts with the oil phase (oil = either hexane or hexane + DEHiBA). The resulting surface was obtained by interpolation between the interfacial grid points. We likewise calculated the surface of water at the interface.

Potential of Mean Force (PMF) calculations. We calculated the Helmoltz free energy profiles $\Delta A(z)$ for interface crossing by selected solutes (L = DEHiBA, the $UO_2(NO_3)_2(L)_2$ or $Eu(NO_3)_3(L)_3$ complexes, the HNO_3 molecule), with either pH neutral or acidic water, using the ESP charges for DEHiBA without polarization (STD model) to retain the study computationally tractable. The position of

dx.doi.org/10.1021/jp4028386 | J. Phys. Chem. B XXXX, XXX, XXX−XXX

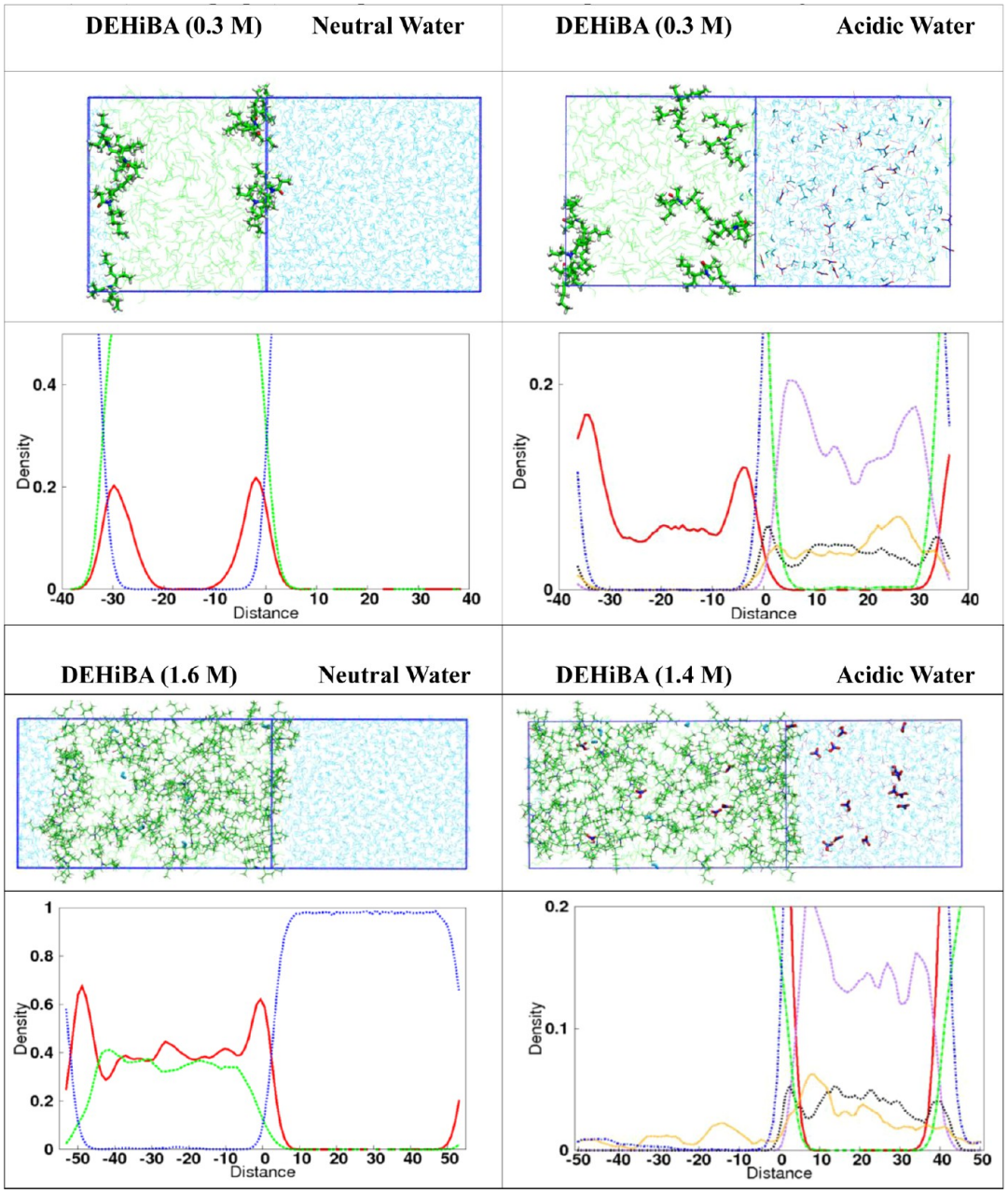

Figure 1. Hexane + DEHiBA/water interface simulated with the POL model. Snapshots after 5 ns and density curves of hexane (green), water (dotted blue), DEHiBA (red), HNO_3 (yellow), H_3O^+ (black), and NO_3^- (purple). Order parameters and H_2O dipoles are shown in Figure S3 in the Supporting Information.

the solute was defined by the z-distance of its center of mass from the interface where $z = 0$. The solute was gradually moved from the interface (initial state $\lambda = 1$) toward the water or the oil phase (final state $\lambda = 0$) up to a z-distance of 20 Å, by steps $\Delta z = 0.5$ Å, i.e., $\Delta\lambda = 0.025$.

$$\Delta A = \int_0^1 \left\langle \frac{\partial U}{\partial \lambda} \right\rangle_\lambda d\lambda \qquad (2)$$

The change in free energy at each step λ was calculated using the thermodynamic integration method (TI) based on eq 2.[42] At each λ step, we performed 0.5 ns of equilibration plus 1.0 ns of data collection and averaging, requiring a total simulated time of 60 ns per PMF. Along the PMF simulation, when the solute is moved away from the interface, the precise z-location of the interface may be somewhat shifted. We thus recalculated the crossing of the solvents density curves at every step of the PMF, and used this updated reference for the $\Delta A(z)$ curves presented here.

QM Calculations. All structures were optimized at the DFT/B3LYP level of theory using the Gaussian09 software.[43] The H, C, N, O atoms of the ligands were described by the 6-31G(d,p) or 6-311+G(d,p) basis set.[43] For the U atom we used the small-core relativistic effective core potential (ECP) of the Stuttgart−Dresden group (SDD) together with their valence basis sets from which each most diffuse s-, p-, d-, and f-function was omitted, affording a [7s6p5d3f] contraction.[44] QM calculations "in aqueous solution" were conducted with the PCM model where the solvent is represented by a polarizable continuum medium with a dielectric constant of

dx.doi.org/10.1021/jp4028386 | J. Phys. Chem. B XXXX, XXX, XXX−XXX

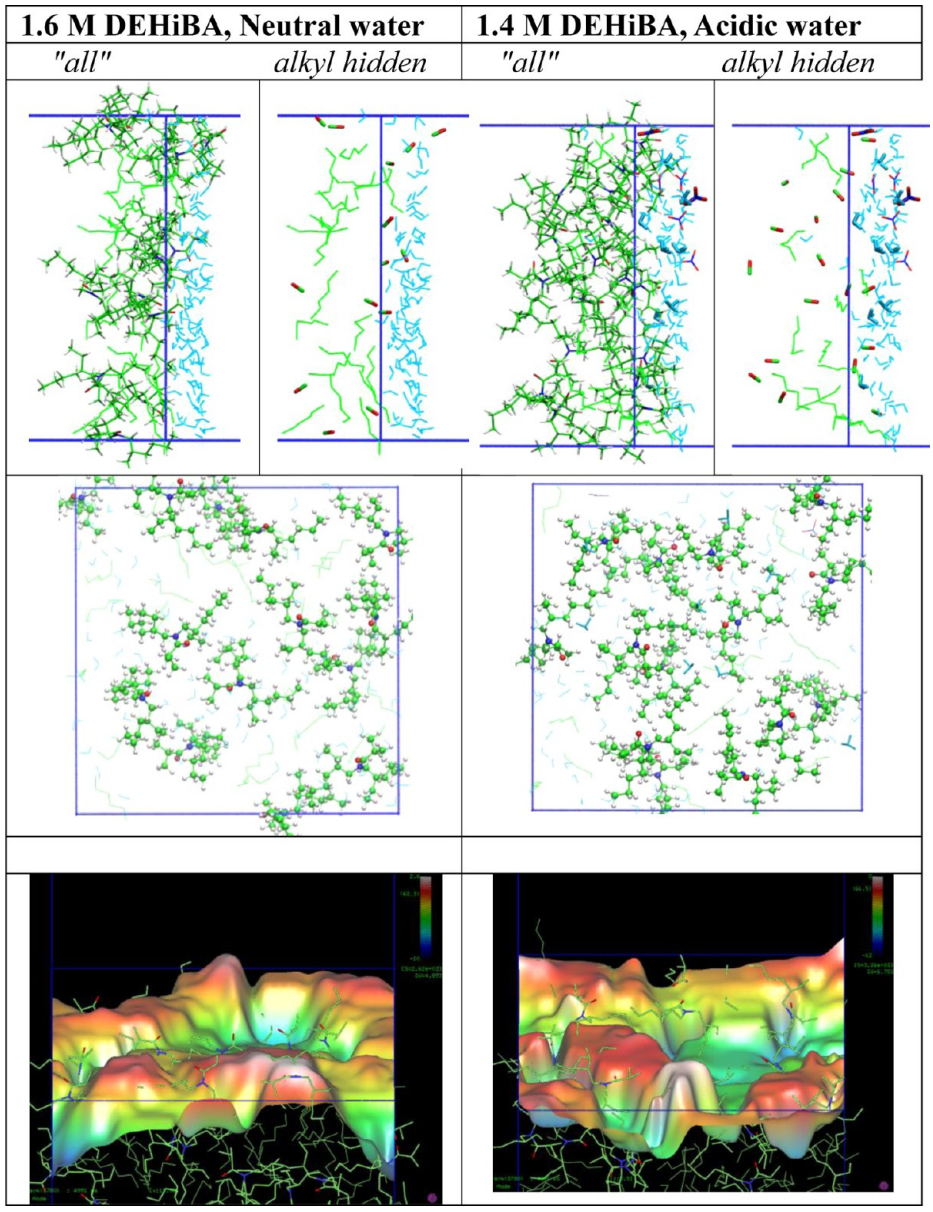

Figure 2. DEHiBA + hexane/water interface with about 1.5 M DEHiBA, simulated with the POL model. Top: two side views of the interface (left: "all" interfacial species; right: *N*-alkyl and alkyl groups of DEHiBA are hidden). Line 2: *xy* plane of the interface. Line 3: perspective view of the interfacial surface (water on the top side). Results with the STD and SCAL models are given in Figures S4 and S6 in the Supporting Information.

80, and the solvent-accessible surface of the solute is calculated from atomic radii of the UFF force field scaled by 1.1.[45]

RESULTS

In the following, we first discuss the MD results on juxtaposed "neat" biphasic systems (without uranyl salt), with neutral and acidic aqueous phases. This is followed by the discussion of free energy profiles for interface crossing by DEHiBA and its $UO_2(NO_3)_2$ and $Eu(NO_3)_3$ complexes and, finally, by the results of "demixing MD experiments" on typical mixtures involved in the uranyl extraction process by DEHiBA.

I. Neat DEHiBA + Hexane/Water Interface with Neutral versus Acidic Water. In all simulated biphasic systems with juxtaposed liquids in an approximate 50:50 water/oil ratio, the two phases remained well separated, delineating two interfaces. In no case did a DEHiBA molecule solubilize in water, while in some cases (with nitric acid, and/or with the SCAL or POL models) a few H_2O and HNO_3 molecules diffused in the oil phase.

The neat interface was studied with pH neutral or acidic water at two DEHiBA concentrations: 0.3 M and about 1.5 M (1.6 M with neutral water and 1.4 M with acidic water). Moreover, two solutions without DEHiBA were simulated as a reference (see Figure S1 in the Supporting Information). Note that the box sizes somewhat differ from one system to the other. Final snapshots and density curves obtained with the POL model that best represents water at the interface are shown in Figure 1. Their features are similar to those obtained without polarization (Figure S2 in the Supporting Information).

dx.doi.org/10.1021/jp4028386 | J. Phys. Chem. B XXXX, XXX, XXX−XXX

At low concentration, the eight DEHiBA molecules, initially placed in the bulk hexane phase, adsorb at the two interfaces during the dynamics (four DEHiBA at each interface) in neutral conditions, indicating that they are surface active, as reflected by the corresponding density peaks with both STD and POL models. When the aqueous phase gets acidified, all DEHiBA's remain adsorbed with the STD model, while with the POL model they dynamically exchange between the interface(s) and the bulk hexane, indicating that they become less surface active: only 3−4 DEHiBA's sit at the interface(s), on the average. At the interface, the carbonyl groups, H-bonded to H_2O molecules, display versatile orientations, yielding order factors of $S \approx 0.6$ in neutral conditions, corresponding to a tilt angle of about 30° with respect to the z-axis, on the average. Note that the positioning of the carbonyls with respect to the water surface forces some alkyl groups of DEHiBA to be immersed in a water microenvironment, which is unfavorable. At the interface, every DEHiBA molecule displays similar attraction energies with the hexane and water phases ($\Delta E_{int} = -19 \pm 1$ and -18 ± 2 kcal/mol, respectively, with the STD charges; see Table S5 in the Supporting Information).

The surface activity of DEHiBA is also observed at the higher concentrations (about 1.5 M), simulated with the POL model or without polarization (STD or SCAL models). With the three models, most of the 60 DEHiBA's are diluted in the hexane phase, but their density d is higher at the interfaces ($d \approx 0.6$) than in the bulk ($d \approx 0.4$). Note that in the concentrated pH neutral or acidic solutions, the interface is not fully covered by the DEHiBA's (see snapshots in Figure 2), presumably due to their bulkiness and low affinity for the interface. The average interfacial area per DEHiBA amounts to 100−104 $Å^2$, with the STD, SCAL or POL models. As expected, the order factor S is close to zero in the bulk oil phase where DEHiBA's adopt "random" orientations, but peaks at the interfaces at 0.6−0.8, depending on the model, as in diluted conditions, indicating that the carbonyls adopt, on the average, similar orientations at the interface at both concentrations.

Water and Acid Extraction. In the reference systems (i.e., without DEHiBA) and in the diluted DEHiBA solutions, neither water nor nitric acid is extracted to the oil phase during the dynamics with the STD or POL models. This contrasts with the 60 DEHiBA's containing systems where water and nitric acid (when present) are extracted, by different amounts depending on the model (see Figures S3 and S5 in the Supporting Information). With the POL model, the number $n_{oil}(H_2O)$ of extracted H_2O species is similar in neutral and acidic conditions (7 and 6 H_2O, respectively; averages during 4−5 ns of dynamics). Note that these numbers are intermediate between those obtained with the STD and SCAL models (2 and 25, respectively in pH neutral systems; 5 and 7, respectively in acidic systems). These features are consistent with the fact that H-bonding interactions of DEHiBA with neutral species (H_2O or HNO_3) are somewhat underestimated with the STD model, and overestimated with the SCAL model (see Table S2 in the Supporting Information).

In all simulated systems, nitric acid is extracted only in its neutral form HNO_3, generally H-bonded to carbonyl oxygens, either directly or via an H_2O molecule. One does not find $OH_3^+\cdots O{=}C$(DEHiBA) adducts in the oil phase that would be analogues of the $OH_3^+\cdots O$(TBP) adducts evidenced with TBP.[32,46] Comparing the three models, one sees, as for the water extraction, that the amount of extracted acid follows the order STD < POL < SCAL model (4, 5, and 6 HNO_3 molecules, respectively).

Nitric Acid at the Interface. At the interface, with the three models, the density of HNO_3 displays a small peak (Figure S5), a feature also observed without DEHiBA (Figure S1). On the average, the number n_{itf} of HNO_3 species within 5 Å from the interface without DEHiBA is 5, 5, and 3, respectively, with the STD, SCAL, and POL models. In the presence of 1.5 M DEHiBA, the corresponding numbers are 4, 4, and 2, respectively. With the three models, there is thus somewhat less undissociated acid with DEHiBA than without, which suggests that HNO_3 is not "attracted" by DEHiBA at the interface. This feature is unlikely to result from force field deficiencies, since the three models qualitatively account for the stronger interaction of DEHiBA with HNO_3 compared to H_2O, as indicated by QM calculations in the gas phase ($\Delta\Delta E \approx 6$ kcal/mol; see Table S2). Furthermore, using "modified" HNO_3 charges that more accurately fit the QM calculated $\Delta\Delta E$ (see Table S2) does significantly change neither the amount of HNO_3 extracted and at the interface nor the DEHiBA solvation at the interface (see, for instance, analysis of trajectories obtained with the POL model in Tables S7−S9 in the Supporting Information).

Looking now at the dissociated form of the acid, one sees that the H_3O^+ density curves overlap with DEHiBA densities in the interfacial region (see dotted black curves and red lines, respectively, in Figure S5), and this feature is most pronounced with the POL model, which might hint at mutual interactions near the interface. There is no such clear evidence, however. The results of statistical analysis of $n_{itf}(H_3O^+)$ ions (see Table S6 in the Supporting Information) within 5 Å from the interfaces depend on the electrostatic model. With the POL model, n_{itf} is similar with DEHiBA and without ($n_{itf} = 9$), supporting the lack of strong H_3O^+ complexation by DEHiBA at the interface (see also Table S7). Similar trends are observed if one considers interfacial slabs of ±7 Å instead of ±5 Å (Table S6). In fact, with neither STD nor POL models are $OH_3^{+\bullet\bullet\bullet}O$(DEHiBA) "complexes" observed at the interface. Such complexes form only with the SCAL model that exaggerates this interaction (see Table S6): in that case, about 1/3 of interfacial DEHiBA's form long-lived (up to 4 ns) complexes with H_3O^+.

The residence times τ_{itf} of acid "at the interface" are quite short (generally less than 100 ps on the average; see Table S6) and depend on the selected Δz width of the interfacial slab and on the electrostatic model. With the POL model, average residence times $\langle\tau_{itf}\rangle$ of HNO_3 are comparable with DEHiBA and without (13 and 20 ps, respectively, for $\Delta z = \pm 5$ Å). Looking at the largest contributions to $\langle\tau_{itf}\rangle$, one sees that some species stay for up to about 300 ps at the interface, while the majority have much shorter lifetimes, illustrating the dynamic nature of the systems. For H_3O^+ ions, the $\langle\tau_{itf}\rangle$ times, similar to those of HNO_3, also remain similar with DEHiBA as without (40−30 ps). Similar features are observed with a wider slab ($\Delta z = \pm 7$ Å), and/or with the STD model, supporting the lack of either HNO_3 or H_3O^+ complexation by DEHiBA at the interface, presumably because of the preferred hydration of both partners (see H-bonds analysis in Table S7). Regarding the interfacial H_3O^+ ions, they adopt with the POL model specific "hydrophobic positioning" (O atom pointing toward the oil phase and O−H bonds rather

dx.doi.org/10.1021/jp4028386 | J. Phys. Chem. B XXXX, XXX, XXX−XXX

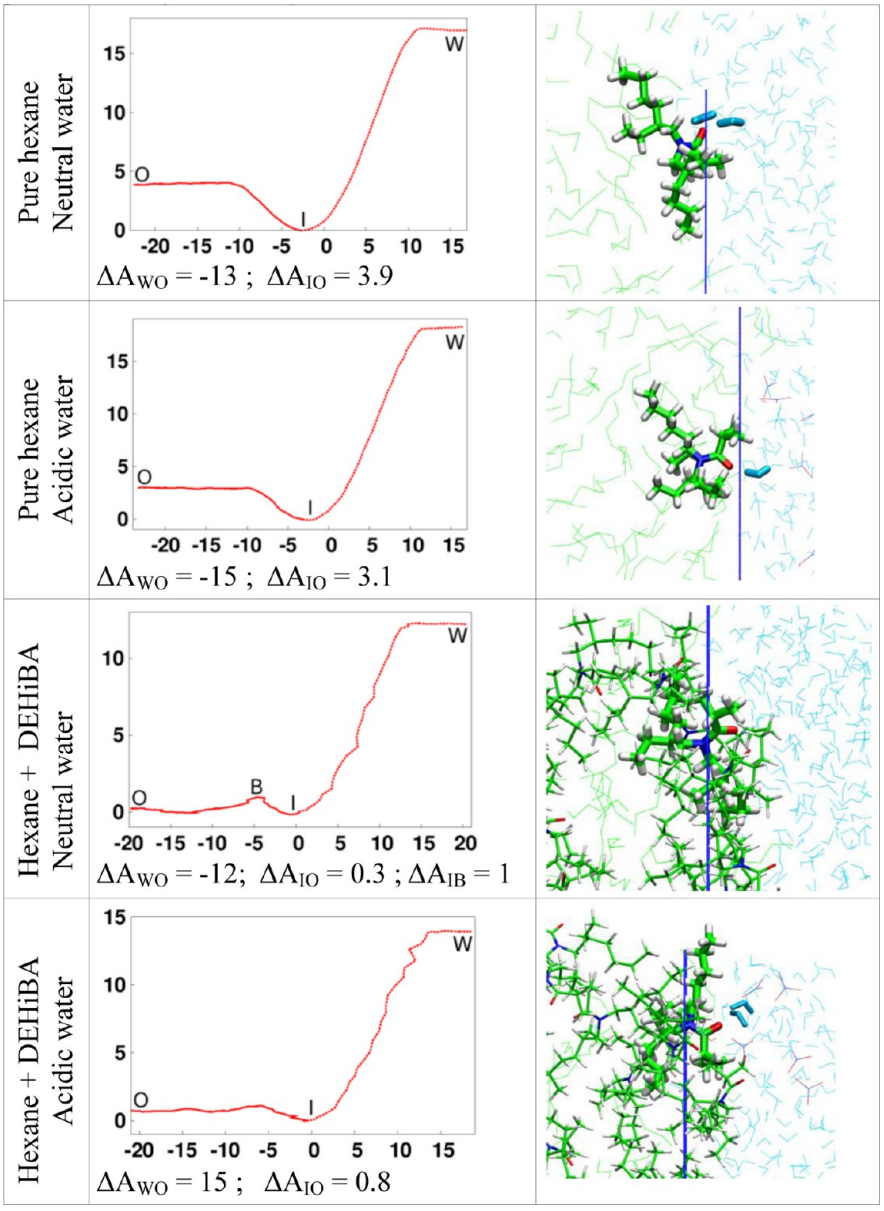

Figure 3. Interface crossing by L = DEHiBA, from neutral or acidic water to pure hexane or to a 59 DEHiBA + hexane solution: free energy profiles (ΔA in kcal/mol, as a function of the z-position, in Å) and typical snapshots at the interface (I position). Snapshots at O, W, and B positions are given in Figure S7 in the Supporting Information.

"tangential" to the interface; see Figure S6)[47,48] in the DEHiBA-containing solution as well as in the reference solution. At the interface and in water, the $H_{H_3O^+}$ protons are mainly solvated by water rather than by HNO_3 molecules or NO_3^- anions (see Table S8 in the Supporting Information). At both positions, the HNO_3 proton mainly interacts with water and NO_3^- oxygens (see detailed analysis in Table S9 in the Supporting Information).

II. Free Energy Profiles for Interface Crossing by DEHiBA and Its Complexes. We calculated the free energy profiles $\Delta A(z)$ for transferring a single DEHiBA molecule (L) or its $UO_2(NO_3)_2(L)_2$ or $Eu(NO_3)_3(L)_3$ complexes across the hexane/water interface, comparing neutral to acidic (3 M nitric acid) aqueous phases. The results are shown in Figure 3 for DEHiBA, and in Figures 4 and 5 for its complexes. All free energy curves display a minimum (I position) between 0 and −5 Å (i.e., on the oil side of the interface), and a plateau in bulk water (W position) and in bulk oil (O position). The energy difference ΔA_{WO} between the bulk phases is quite high (−12 to −26 kcal/mol), indicating that these species are hydrophobic and partition to the oil phase, following experimental observations.

Transfer of the Uncomplexed DEHiBA. The PMF of a DEHiBA molecule has been simulated with two compositions of the oil phase: either neat hexane ("high DEHiBA dilution"), or with a concentrated solution (1 + 59 DEHiBA) in hexane, to investigate how these modify the interfacial energy landscape. In fact, without acid, the energy minimum (ΔA_{IO} = 3.9 kcal/mol) observed at the interface at high dilution nearly disappears (ΔA_{IO} = 0.3 kcal/mol) when DEHiBA's gets more concentrated, because the interface gets more or less covered by other DEHiBA molecules (vide supra), thereby reducing the interfacial tension (see, for example, calculated values in Table S10 in the Supporting

dx.doi.org/10.1021/jp4028386 | J. Phys. Chem. B XXXX, XXX, XXX−XXX

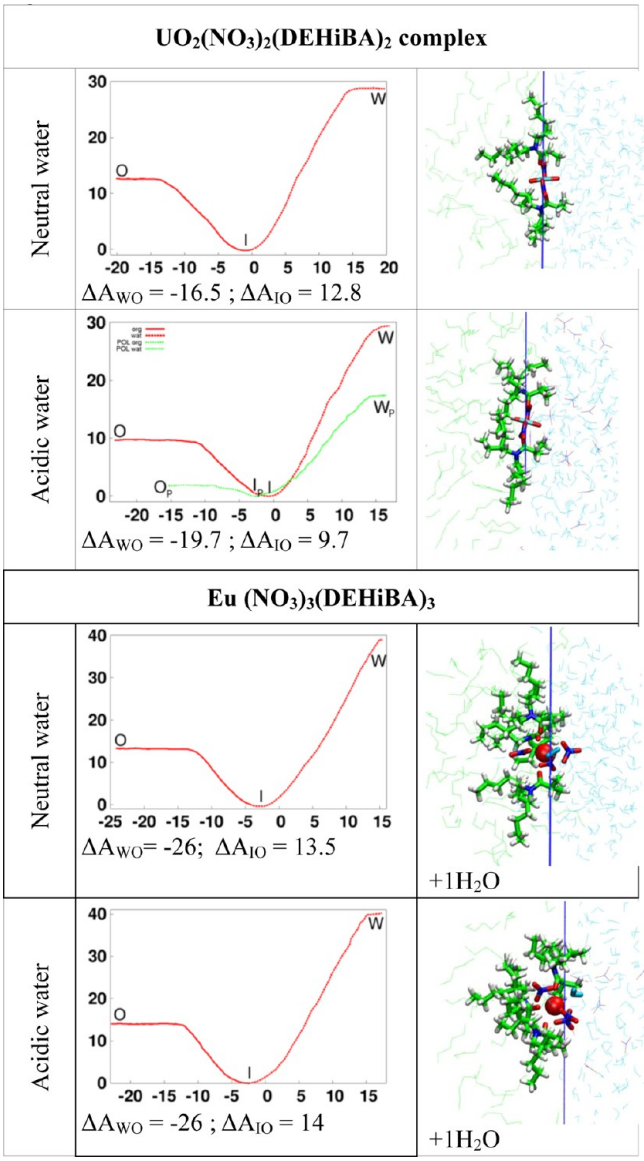

Figure 4. Interface crossing by the $UO_2(NO_3)_2(L)_2$ and $Eu(NO_3)_3(L)_3$ complexes from neutral or acidic water to the oil phase (L = DEHiBA): free energy profiles (ΔA in kcal/mol) and typical snapshots at the interface. The red curves are obtained with the STD model, while the green curve is obtained with the POL model. Snapshots at O and W positions are shown in Figures S8 and S9 in the Supporting Information.

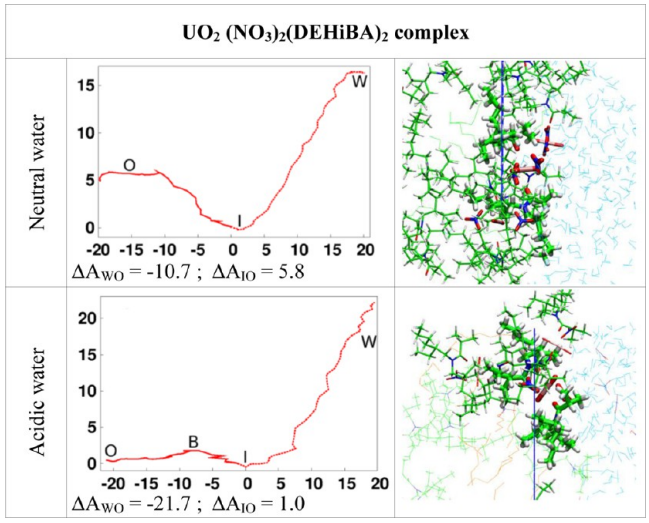

Figure 5. Interface crossing by the $UO_2(NO_3)_2(DEHiBA)_2$ complex from neutral or acidic water to the oil phase (hexane + 40 DEHiBA + 4 complexes): free energy profiles (ΔA in kcal/mol) and typical snapshots at the interface (I position). Snapshots at positions O, B, and W are shown in Figure S10 in the Supporting Information.

Information) and the surface activity of DEHiBA. Similar features are observed in acidic conditions: the free energy difference ΔA_{IO} decreases (from 3.1 to 0.8 kcal/mol) when DEHiBA gets concentrated in the oil phase. Furthermore, adding acid somewhat increases the ΔA_{WO} energy difference between the two bulk phases (by 2−3 kcal/mol at both DEHiBA concentrations), in keeping with some salting-out effect of the acid.

Looking at the DEHiBA environment at the interface in both diluted and concentrated systems (Figure 3), one sees that its carbonyl oxygen is solvated by 1−2 H_2O molecules, in either neutral or acidic conditions. Furthermore, as mentioned above, some alkyl groups of DEHiBA are "immersed" in water, and this feature mainly occurs for the smallest groups (isopropyl), while the more hydrophobic ethylhexyl chains are generally surrounded by hexane molecules, and/or *N*-alkyl groups of other DEHiBA's (when present). In the oil phase contacted with neutral or acidic water, DEHiBA is solvated by hexane in diluted systems, and by a mixture of other DEHiBA's and hexane in the concentrated system, without displaying specific interactions with the other DEHiBA's, though.

Transfer of the DEHiBA Complexes with Uranyl or Europium Nitrates. The PMF of the $UO_2(NO_3)_2(L)_2$ and $Eu(NO_3)_3(L)_3$ complexes from neutral or acidic water to neat hexane (Figure 4) display marked minima at ≈−2 Å from the interface (I position), and these are deeper than for the free ligand: the ΔA_{IO} energy difference ranges from 10 to 14 kcal/mol, indicating a clear affinity of the complexes for the interface. At the I position, the complexes are indeed more attracted by water ($\Delta E_{int} \approx -62$ to -116 kcal/mol) than by the organic phase ($\Delta E_{int} \approx -36$ to -47 kcal/mol; Table S5). Snapshots (Figure 4) indicate that this "amphiphilic behavior" results from a peculiar positioning of the complexes, whose ligands sit in the oil phase (as for DEHiBA itself), while the uranium or europium nitrate moieties sit "right in the plane of the interface", attracted by water. As a result, O═U═O orients nearly parallel to the *z*-axis while nitrate ligands are parallel to the interfacial plane, as observed for the $UO_2(NO_3)_2(TBP)_2$ analogue.[25] Also notice, as for the free DEHiBA, that the two ligands of the uranyl complex have their shorter (*i*Pr) chains in water, while the ethylhexyl ones sit either in oil or tangential to the interface. Analogous features are observed at the interface for the $Eu(NO_3)_3(L)_3$ complex that cannot adopt such a symmetrical arrangement, however, due to its 3-fold type symmetry. Among its three nitrates, two point toward water, and one points toward the oil side of the interface. Because of its higher ionic content, compared to the uranyl complex, the europium complex has stronger attractions with water ($\Delta E_{int} \approx -115$ and -60 kcal/mol, respectively, at the interface; see Table S5).

Comparing now the free energy profiles of the complexes with +2 versus +3 charged cations, one sees that both complexes have comparable affinities for the interface when

dx.doi.org/10.1021/jp4028386 | J. Phys. Chem. B XXXX, XXX, XXX−XXX

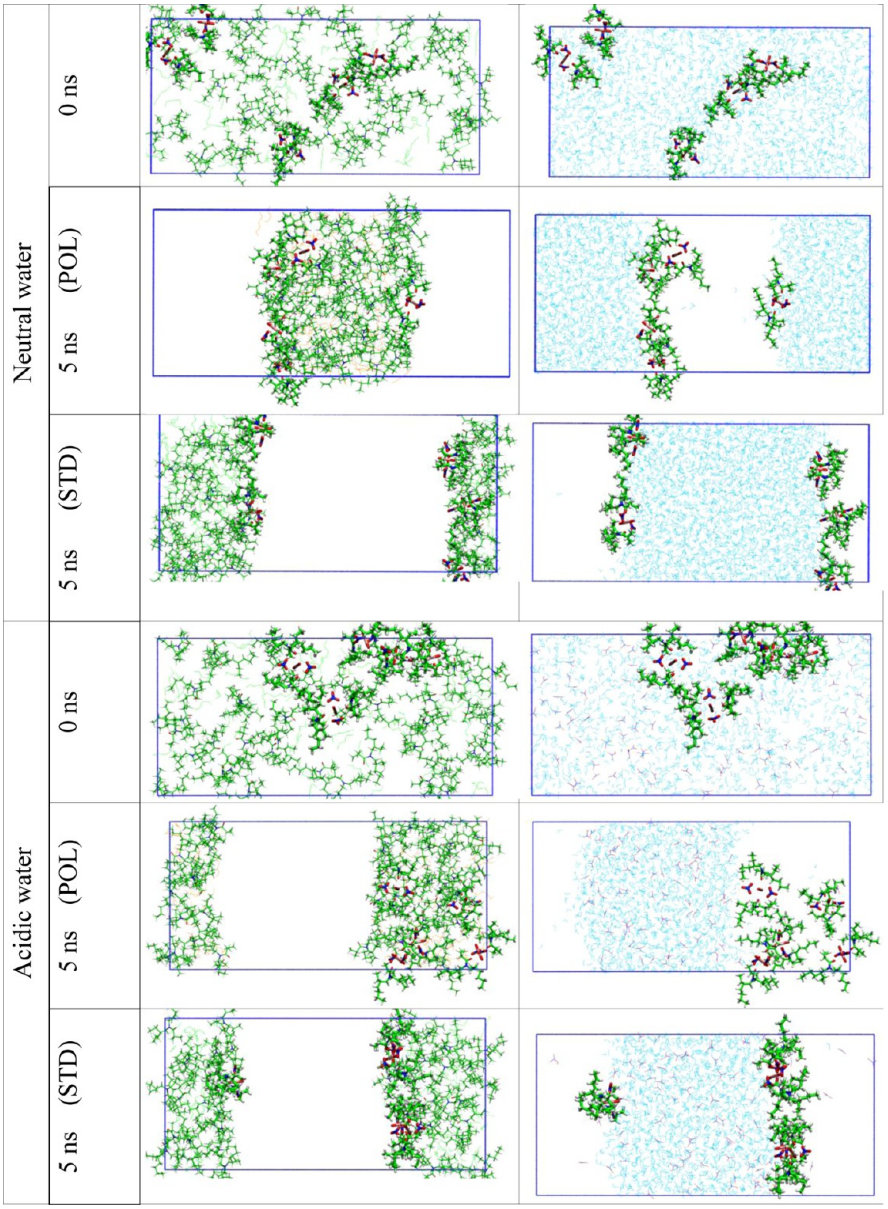

Figure 6. Demixing simulations of a mixture of neutral or acidic water/hexane/40 DEHiBA/5 $UO_2(NO_3)_2(DEHiBA)_2$ (~50:50 oil/water ratio) using the STD and POL models. Snapshots at the beginning and at the end of the dynamics, with oil (left) and water (right) represented separately.

the aqueous phase is neutral (ΔA_{IO} = 12.8 and 13.5 kcal/mol, respectively), due to antagonistic contributions: increased attractions of polar moieties (cation and nitrates) with water, but higher hydrophobic features when the number of DEHiBA ligands increases from 2 to 3. In acidic conditions, the europium complex becomes more surface active than the uranyl complex (ΔA_{IO} = 14.0 and 9.7 kcal/mol, respectively), because the former cocomplexes 1 H_2O molecule at the interface as in the bulk water or oil phases. In no case are NO_3^- or H_3O^+ ions extracted to the organic phase along the PMF simulations.

Acidifying the aqueous phase and adding solutes in the oil phase (40 DEHiBA plus 4 $UO_2(NO_3)_2(L)_2$ complexes) to model more realistic extraction conditions markedly modifies the energy profile for transferring one complex (see Figure 5): migration from the interface to water remains a high-energy process (ΔA_{IW} > 22 kcal/mol), whereas migration from the interface to the bulk oil phase is facilitated: there is a tiny minimum at the interface, at only 1.0 kcal/mol lower in energy compared to the bulk oil, and the two positions are separated by a small barrier (ΔA_{IB} = 2.3 kcal/mol). Note that along the PMF simulations of 60 ns in either acidic or neutral conditions, the four $UO_2(NO_3)_2(L)_2$ complexes that were free to move remain at the interface.

All PMF curves discussed above have been obtained with the STD model. To gain insights into the effect of polarization, we decided to recalculate the PMF of the $UO_2(NO_3)_2(L)_2$ complex at the water/hexane interface, using the computationally more demanding POL model. The results (green curve in Figure 4) confirm the surface activity of the complex and its preference for the oil phase over the aqueous phase. However, the ΔA_{IO} energy (1.8 kcal/mol) is much lower than with the STD model (9.7 kcal/mol), indicating that explicit account of polarization effects reduces the surface

dx.doi.org/10.1021/jp4028386 | J. Phys. Chem. B XXXX, XXX, XXX−XXX

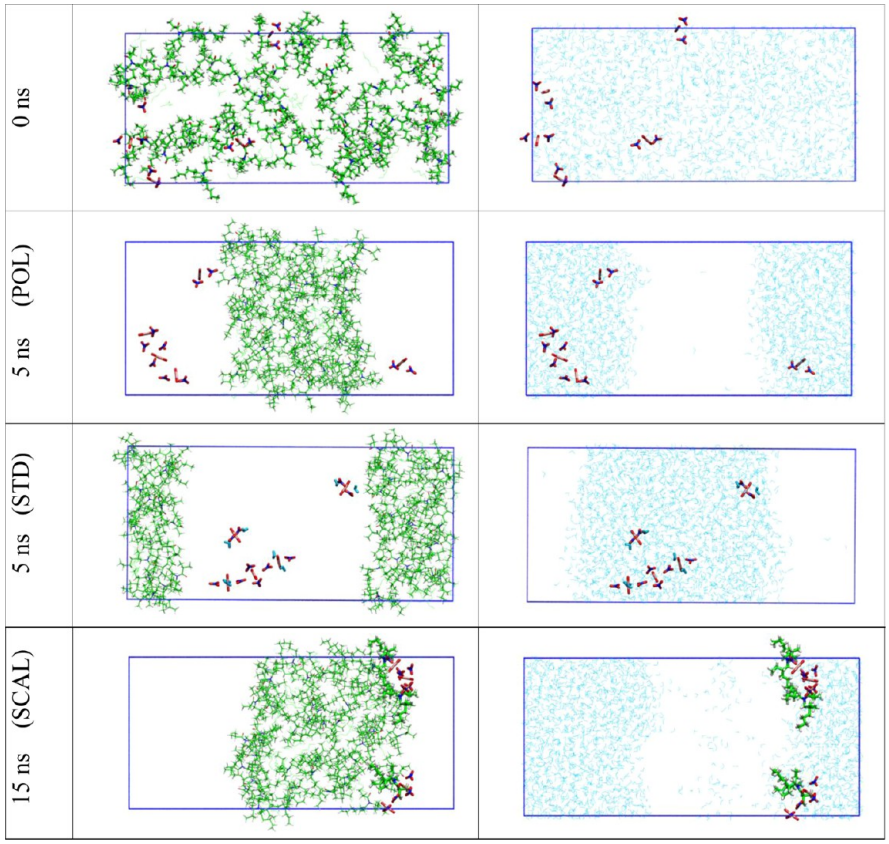

Figure 7. Demixing simulations of a mixture of neutral water/hexane/50 DEHiBA/5 $UO_2(NO_3)_2$ (~50:50 oil/water ratio) using the STD, POL, and SCAL models. Snapshots at the beginning and at the end of the dynamics, with oil (left) and water (right) represented separately. Additional demixing MD tests on this system are given in Figure S13 in the Supporting Information.

activity of the hydrophobic neutral complex. Furthermore, the ΔA_{OW} energy difference between the bulk phases decreases (from 19.7 kcal/mol with the STD model to 15.6 kcal/mol with the POL model). In fact, with the POL model, the dipole moment μ_{H_2O} of POL3 water becomes lower at the water surface than in bulk water ($\mu_{H_2O} \approx 2.2$ and 2.6 D, respectively, at the water/CCl_4 interface[49,50]), and lower than with TIP3P water (2.35 D), somewhat diminishing the attraction of interfacial water with the polar moieties of the solutes. Likewise, in bulk water, the solvation energy of $UO_2(NO_3)_2(L)_2$ diminishes from the STD model in TIP3P water, to the POL model in POL3 water.

III. Demixing Simulations of "Randomly Mixed" Uranyl Nitrate, DEHiBA's, Water, and Oil: Phase Separation and Uranyl Complexation. In this section, we report the results of MD demixing simulations of random mixtures of water, hexane, and a total of 50 DEHiBA molecules, in neutral or acidic conditions, with either complexed or uncomplexed uranyl nitrate. First, we consider the preformed $UO_2(NO_3)_2(L)_2$ complexes using the STD and POL models to compare their partitioning with the one predicted from the PMF simulations without polarization. We then consider mixtures with uranyl nitrate to investigate whether uranyl will be complexed by DEHiBA (and ultimately will be extracted) when the phases separate. This will be achieved at two oil/water ratios: about 50:50 as above, and 90:10 to model oil-rich mixtures (as occurring upon macroscopic phase separation, e.g., upon centrifugation). In most cases, the demixing has been simulated for at least 5 ns with the three electrostatic models.

1. Demixing of 50:50 Oil–Water Mixtures and Complexed versus Free Uranyl Nitrate. Solutions with $UO_2(NO_3)_2(L)_2$ Complexes. A first question we addressed by the demixing simulations deals with the partitioning of the preformed $UO_2(NO_3)_2(L)_2$ complexes: are they extracted to the oil phase during the dynamics, as experimentally observed after phase separation? In fact, when the randomly mixed solution contains five $UO_2(NO_3)_2(L)_2$ complexes and an excess of free ligands, with either neutral or acidic water, the two phases demix rapidly during the dynamics with either STD or POL models (see Figure 6, and Figure S11 in the Supporting Information). After 5 ns, the two phases are completely separated, delineating "planar" interfaces (as in simulations of juxtaposed solvent boxes), onto which the complexes (all five complexes with the STD model and four complexes with the POL model) adsorb in an amphiphilic manner when water is neutral. This is consistent with the PMF results reported above with the STD model "at high DEHiBA dilution" and for the concentrated systems. For the acidic system, one also finds more complexes at the interface without polarization (all five complexes) than with polarization (only two complexes adsorb at the interface, while the three others sit in the oil phase and are thus "extracted"). Comparing the POL results with and without acid shows that acid reduces the affinity of the neutral complexes for the interface and favors extraction, as observed experimentally. This is also consistent with PMF results reported above without polarization. In no case are H_3O^+ or NO_3^- ions

dx.doi.org/10.1021/jp4028386 | J. Phys. Chem. B XXXX, XXX, XXX−XXX

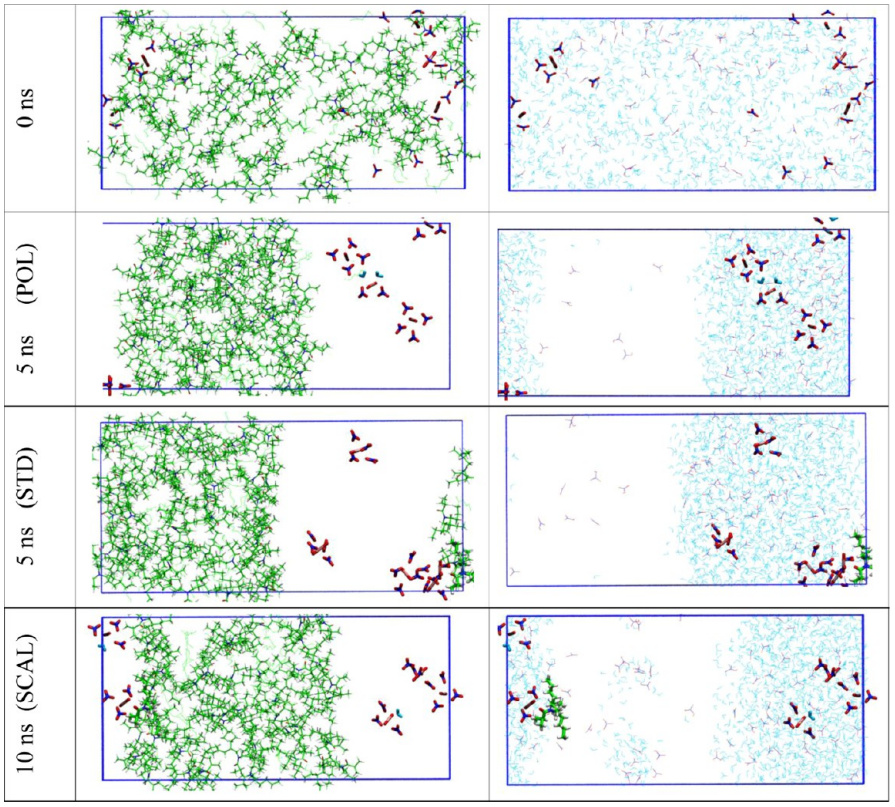

Figure 8. Demixing simulations of a mixture of acidic water/hexane/50 DEHiBA/5 $UO_2(NO_3)_2$ (~50:50 oil/water ratio) using the POL, STD, and SCAL models. Snapshots at the beginning and at the end of the dynamics with oil (left) and water (right) represented separately.

found in the oil phase, since nitric acid is extracted in its HNO_3 form only (3 species with the POL model, 5 species with the STD model).

Solutions with Uncomplexed Uranyl Nitrate. Simulating the spontaneous complexation of uranyl by DEHiBA is a more challenging task, due to force field limitations and sampling issues, especially when there are no strong driving forces for complexation. Previous simulations of TBP/oil/water mixtures with uranyl nitrates led, however, to the formation of 1:2 and 1:1 complexes, namely $UO_2(NO_3)_2(TBP)_2$ and $UO_2(NO_3)_2(TBP)$, respectively.[24,32,51] In the demixing simulations of DEHiBA with the STD or POL models no such complexes form, however (see Figure 7, and Figure S13 in the Supporting Information). After 5 ns, all $UO_2(NO_3)_2$ species sit in water, without contact with interfacial ligands, preventing further complexation. Repeating the demixing simulation, but using scaled charges on DEHiBA (SCAL model) yields a different outcome regarding phase separation and complexation. The more polar DEHiBA is less hydrophobic and, as a result, there is no complete phase separation after 5 ns of dynamics. At that stage, the oil domain is quite elongated, delineating an "horizontal" interfacial domain (Figure S12 in the Supporting Information), of higher (and hence less stable) surface than the "vertical" area obtained with STD model. When the dynamics is pursued up to 10 ns, the phases rearrange, without forming "flat" interfaces, though. One finds an irregular cylindrical hexane + DEHiBA domain, surrounded by water. The interesting feature is that four of the five $UO_2(NO_3)_2$ species now sit near the oil surface, complexed by DEHiBA, forming 1:1 adducts further coordinated to 1 H_2O molecule. These $UO_2(NO_3)_2(L)(H_2O)$ species are more polar, less hydrophobic, and hence more surface active that the 1:2 $UO_2(NO_3)_2(L)_2$ complexes.

When water gets acidified, the aqueous and oil phases separate in less than 5 ns (Figure 8). With the STD and POL models, no uranyl is complexed by DEHiBA during the dynamics. With the SCAL model (Figure S14 in the Supporting Information), the resulting interface is more irregular than with the STD or POL models, and one uranyl gets complexed to form the anionic $UO_2(NO_3)_3(L)^-$ species with one additional monodentate nitrate ligand. The other $UO_2(NO_3)_2$ species captured nitrates to form $UO_2(NO_3)_4^{2-}$ or $UO_2(NO_3)_3^-$ adducts, with the three models.

2. Demixing of Oil-Rich Water Mixtures with Uncomplexed Uranyl Nitrate. The lack of uranyl complexation by DEHiBA in most 50:50 mixtures led us to consider solutions where oil is in excess over water (90:10 ratio) to investigate whether complexes form in neutral or acidic conditions, comparing the three electrostatic models. In principle, reducing the amount of water should favor the complexation and extraction of uranyl nitrate, but the results are not so simple.

Let us first consider the pH neutral solutions (without acid). Snapshots after 5 ns of demixing dynamics are shown in Figure 9, and Figure S15 in the Supporting Information. With the STD or POL models, the two liquids are well separated, and water is confined in a cylindrical domain, mostly surrounded by DEHiBA's. With both models, the five $UO_2(NO_3)_2$ species sit near the core of the water pool and have their equatorial shell completed by 2 H_2O ligands. They have no direct contact with the oil surface, thus preventing complexation by DEHiBA. These features differ from those obtained with the SCAL model. In that case, there is no full

dx.doi.org/10.1021/jp4028386 | J. Phys. Chem. B XXXX, XXX, XXX−XXX

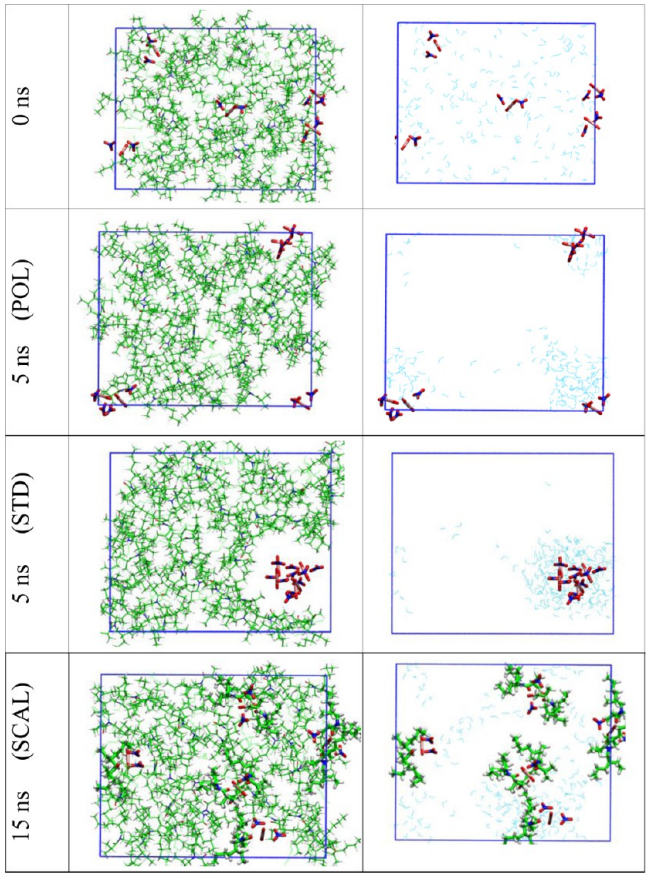

Figure 9. Demixing simulations of a mixture of neutral water/hexane/50 DEHiBA/5 $UO_2(NO_3)_2$ (~90:10 oil/water ratio) using the POL, STD, and SCAL models. Snapshots at the beginning and at the end of the dynamics with oil (left) and water (right) represented separately.

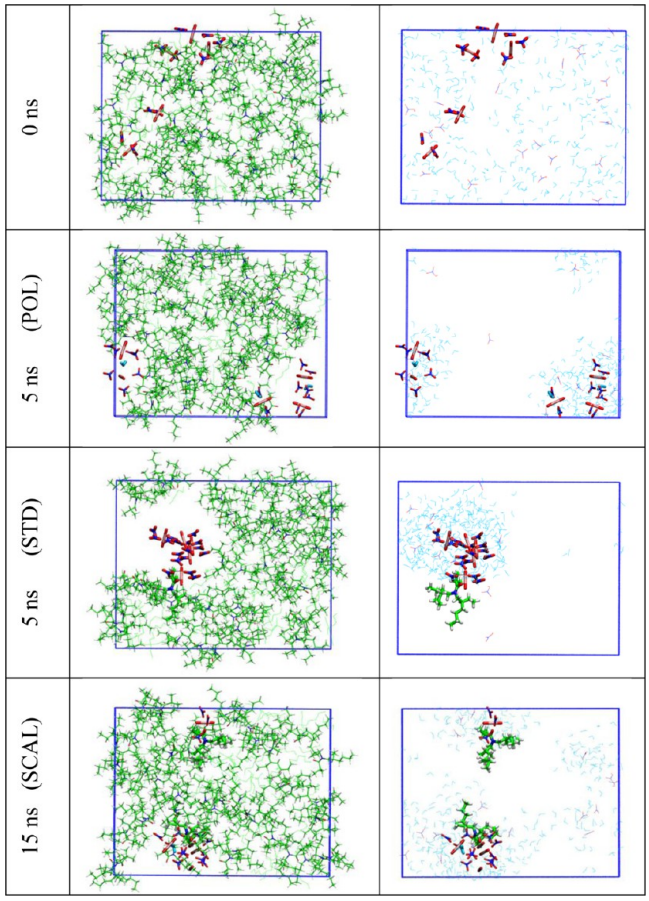

Figure 10. Demixing simulations of a mixture of acidic water/hexane/50 DEHiBA/5 $UO_2(NO_3)_2$ (~90:10 oil/water ratio) using the POL, STD, and SCAL models. Snapshots at the beginning and at the end of the dynamics with oil (left) and water (right) represented separately.

phase separation after 5 ns of demixing, but one can see water-rich domains containing uranyl nitrates and two 1:1 plus two 1:2 complexes with DEHiBA. This simulation was pursued up to 15 ns, during which no major solvent reorganization occurred, but all uranyl nitrate species complexed DEHiBA and sometimes water to form finally three $UO_2(NO_3)_2(L)_2$, one $UO_2(NO_3)_2(L)(H_2O)$, and one $UO_2(NO_3)_3(L)(H_2O)^-$ species (whose monodentate nitrate belongs in fact to a neighboring uranyl complex). Noteworthy is the spontaneous formation of the neutral 1:2 complex known to be extracted to the oil-rich phase.

We now turn to the demixing of acidic oil-rich systems that are in principle most relevant since uranyl extraction experimentally proceeds from nitric acid solutions. Final snapshots are shown in Figure 10. As observed for neutral water, simulations of acidic systems with STD and POL models lead to well-separated water and oil domains whereas with SCAL model there is no full phase separation, even after 15 ns. Regarding uranyl nitrate, different complexation scenarios are observed, depending on the model. With the STD model, one $UO_2(NO_3)_2$ species complexed a DEHiBA and a nitrate to form UO_2 $(NO_3)_3(L)^-$, while the other $UO_2(NO_3)_2$ species captured two nitrates in their equatorial shell, forming $UO_2(NO_3)_4^{2-}$. With the POL model, all $UO_2(NO_3)_2$ species completed their equatorial shell by 2 NO_3^- or H_2O ligands, without complexing DEHiBA. With the SCAL model, two $UO_2(NO_3)_3(L)^-$ complexes formed while the remaining $UO_2(NO_3)_2$ species cocomplexed 2 NO_3^- or 1 NO_3^- plus 1 H_2O (see also Figure S16 in the Supporting Information).

DISCUSSION

We report MD investigations of the liquid−liquid interfacial landscape involved in the extraction of uranyl nitrate by the hydrophobic amide ligand, from an aqueous phase (either pH neutral or acidic) to an oil phase (either pure hexane or hexane + DEHiBA, in an approximate 3:1 volumic ratio, as used experimentally). Initial reference systems (without uranyl) are studied from juxtaposed liquids, whereas uranyl containing systems are simulated starting from random mixtures to enhance the sampling (demixing simulations). Insights into the free energies for interface crossing by DEHiBA in its free and complexed states, in ideal conditions (neat water and oil phases), and more realistic conditions (with added nitric acid, and DEHiBA added as cosolvent in the oil phase) are also presented, based on PMF simulations.

1. Computational Aspects. On the methodological side, we compare MD results obtained with three electrostatic representations of the system: the STD and SCAL models are based on pairwise additive 1−6−12 interactions between the atoms, with either "standard" (ESP) charges or with more polar "scaled charges" on DEHiBA. The third model POL that uses atomic polarizabilities from the literature is a priori

dx.doi.org/10.1021/jp4028386 | J. Phys. Chem. B XXXX, XXX, XXX−XXX

more satisfactory to simulate liquid−liquid interfaces where, among others, the interfacial water molecules are less polar than in the bulk.[49,50] Polarization is also important to depict ions at aqueous interfaces.[52−57] Regarding the SCAL model where ESP charges of DEHiBA were scaled by 1.5 to possibly observe "spontaneous" complexation of uranyl nitrate, it somewhat exaggerates its polarity and its interactions with uranyl nitrate, water, HNO_3, or H_3O^+ species (see Table S2). In the gas phase, the interaction energies of DEHiBA with neutral species (H_2O, HNO_3, $UO_2(NO_3)_2$) are similar with both STD and POL models and in the range of QM values, while interactions with charged species (H_3O^+, UO_2^{2+}), underestimated with the STD model, are improved with the POL model. None of these models can be the panacea. The POL model is the most appealing, but deserves parameter testing on, among others, polarizability and fixed charges of all species. A good model should account for specific pair interactions (H-bonds, ligand−cation, cation−anion) including nonadditive effects, as well as for thermodynamic features like free energies of adsorption at the interface and free energies of transfer of extractant molecules and their complexes from water to oil. We have seen that hydrophobic species like the $UO_2(NO_3)_2L_2$ complex are less surface active with the POL than with the STD model. Experimental references for such systems are unfortunately lacking. Furthermore, on the practical side, the POL model is presently computationally too demanding to us to perform consistent PMF comparisons of the different studied systems that require long sampling. The representation of ionic species with integer charges (like +2 uranyl, −1 nitrate, +1 proton) that neglect charge-transfer effects may also be a critical issue, as shown for aqueous solutions of simple electrolytes.[58] Our results cannot thus pretend to be quantitative, but overall yield converging views of interfacial features of this extraction system. In the following, we discuss the nature of the "interface", the question of acid extraction, and the relevance of the results for the extraction mechanism.

2. On the Nature of Interface: Size, Composition, and Dynamics. Because the interface between oil (dodecane + DEHiBA) and water (neutral or with nitric acid) has been investigated recently by SHG (second harmonic generation) surface spectroscopy and interfacial tension measurements,[20] some characteristics of the simulated (nano)interfaces are worth discussing. There is no unique definition of the "interface".[59] The Gibbs surface, dynamically defined as a fictitious flat surface positioned at the intersection of the density curves of the two liquids at rest, can serve as a reference ($z = 0$). Note that considering the densities of water and hexane in the case of concentrated DEHiBA solutions can be somewhat misleading, because DEHiBA is both a cosolvent and surface active molecule. As seen from the density curves and snapshots (Figures 1 and 2), hexane tends to be pushed away from the interface by the adsorbed DEHiBA's. This is why using the density of hexane + DEHiBA instead of hexane alone may yield a more appropriate reference for $z = 0$. To "measure" the width of the interface from the densities, we calculated the distance Δz_{90} between z-positions where the water and hexane + DEHiBA densities reach 90% of their bulk values, respectively. The resulting Δz_{90} width is rather small and depends on the electrostatic model: for pH neutral systems, $\Delta z_{90} \approx 3.8$, 5.4, and 7.8 Å, respectively, with the STD, POL, and SCAL models. For the acidic systems, the widths are comparable: $\Delta z_{90} \approx 4.6$, 4.6, and 6.6 Å, respectively.

Due to the granularity of the solvents and of the amphiphilic solutes, the interface is rough, irregular and dynamics. See, for instance, snapshots in Figures S17 and S18 in the Supporting Information, representing the surface of water, color coded as a function of its z-position, at different times. In the case of acidic systems, the Δz difference between extreme positions is 9.7, 8.5, and 13.2 ± 1.5 Å, respectively, with the STD, POL and SCAL models. These numbers are nearly twice larger than the Δz_{90} values reported above, and also increase when the DEHiBA charges are scaled up by 1.5 (from the STD to the SCAL model). Note that, near the interface, H_2O molecules tend to adopt "hydrophobic orientations"[60] and to align their OH dipoles rather tangential to the interface, as seen by the plot of the average $\mu_{H_2O}(z)$ dipole moments (see, e.g., Figures S2 and S5). These are modulated by the DEHiBA and acid content, and by the electrostatic model.

To estimate the interface roughness R, we calculated the "real interfacial area" S_{itf} as defined in the Methods section, and $R = S_{itf}/xy$. R was averaged from the saved trajectories, first without DEHiBA as a reference, then with concentrated DEHiBA, in either neutral or acidic conditions, with the three electrostatic models. The results (Table S11 in the Supporting Information) show that R values are the smallest and have the weakest fluctuations for the neat hexane/water system without acid ($R = 1.60 \pm 0.08$), and that R slightly increases upon addition of 3 M nitric acid ($R = 1.67 \pm 0.10$). When DEHiBA is dissolved in the oil phase, the roughness increases, in the order of simulated models: STD < POL < SCAL. The highest R values and fluctuations are observed for the acidic system simulated with scaled charges ($R = 2.70 \pm 0.40$). Furthermore, the calculated roughness depends on the definition of the oil phase, i.e., either the solvent only (hexane), or the solvent + cosolvent (hexane + DEHiBA). For instance, for the acidic solutions simulated with the POL model, $R = 2.20$ or 1.80, respectively, with these two definitions. The R numbers should thus not be over-interpreted due to the somewhat arbitrary definition of "interfacial" solvent molecules, excluding those that are locally "extracted" (i.e., sitting in the interfacial slab but without direct connection with their bulk phase), or fully extracted (e.g., H_2O in oil).

3. Nitric Acid Extraction to the Oil Phase. The nitric acid and water uptake by DEHiBA has been studied experimentally at different concentrations with dodecane as organic solvent.[20,31,61] For instance, at [DEHiBA] = 1 M and $[HNO_3]_{tot}$ ranging from 2.2 to 6.3 M, acid is extracted with a distribution coefficient of 0.17. The distribution coefficients obtained in our study at a higher DEHiBA concentration (1.6 M) are in this order of magnitude and somewhat larger (about 0.20, 0.25, and 0.30, respectively, with the STD, POL, and SCAL models). Experimentally, the amount of extracted water increases with the total acid concentration and, at $[HNO_3]_{tot} = 3$ M, $[H_2O]_{org} \approx 0.25$ M, which is in the order of magnitude, but larger than the concentrations we obtain ($[H_2O]_{org} \approx 0.12$, 0.17, and 0.19 M, respectively, with the STD, POL, and SCAL models). Experimentally, the ratio $[H_2O]_{org}/[HNO_3]_{org}$ has been varied and shown to be close to 1.0 at low acid concentration, and to decrease to 0.51 at $[HNO_3] = 3$ M and to 0.19 at $[HNO_3] = 6$ M). These

dx.doi.org/10.1021/jp4028386 | J. Phys. Chem. B XXXX, XXX, XXX−XXX

features hint at somewhat stronger interactions of DEHiBA with HNO_3 than with H_2O in the oil phase, as supported by QM results using DMAA as a model, and by the AMBER results with DEHiBA (see Table S2) in the gas phase. At the simulated interfaces, however, we do not find evidence for either HNO_3 or H_3O^+ complexation by DEHiBA with the STD or POL models.

To further investigate the energetics of acid migration from bulk water to the oil phase, we calculated the PMF for interface crossing by a HNO_3 molecule at two DEHiBA concentrations (0.3 and 1.4 M) with 3 M nitric acid in water (see Figure S19 in the Supporting Information). In both cases, a small energy minimum is found at the interface, supporting the weak surface activity of HNO_3. Furthermore, HNO_3 prefers water over oil, but the ΔA_{WO} difference decreases (from 2.6 to 0.1 kcal/mol) when [DEHiBA] is increased, in qualitative agreement with the experimentally observed trends.[31,61]

Because acid extraction has been followed experimentally as a function of time by titration and by SHG spectroscopy,[20] we looked in more detail how extraction occurs along the dynamics of the nanoscopic solutions. First, by counting the number of extracted species as a function of time (Figure S20 in the Supporting Information), one sees that extraction is first rapid and reaches a plateau at 5 ns, hinting at an equilibrated system. This feature is also supported by examination of the POL trajectories at the computer graphics system, indicating that during the 5 ns dynamics, HNO_3 molecules exchange between water and oil, and vice versa. An illustration of HNO_3 extraction is given in Figure S20, representing the trajectory of a molecule that migrates from the aqueous to the organic phase. With the three electrostatic models, HNO_3 diffuses rapidly in both phases. In the bulk water and oil phases, typical diffusion coefficients D (in Å^2/ps, averaged over 1 ns; see Table S12) are, on the average, 0.31 and 0.13, respectively, with the STD model, 0.26 and 0.09, respectively, with the SCAL model, and 0.26 and 0.21, respectively, with the POL model. Diffusion is thus somewhat slower in the oil phase than in water. Interestingly, similar D values are found for HNO_3 and H_2O molecules in a given phase, supporting their high diffusion. This presumably stems from the fact that, even when they are H-bonded to DEHiBA in the oil phase, the HNO_3 or H_2O species remain poorly solvated and jump from one carbonyl to the other.

Experimentally, acid extraction involves time scales (hours) far beyond the simulated ones, and different kinetic regimes.[20] Although no clear molecular pictures of the different steps could be obtained from experiment, it has been proposed that DEHiBA might "complex" the acid at the interface at the early extraction stage.[20] This feature is not supported by our results obtained with a simple force field representation of the acid. Clearly, further studies are needed to characterize the state of the proton in the different environments. For instance, nitric acid is considered as mainly dissociated in bulk water, but an abrupt change has been evidenced when its concentration reaches 4 M.[62] Furthermore, coming to the "water edge", nitric acid should behave as a weak acid,[63] with possible further modulations in the presence of weak bases like DEHiBA. Another issue concerns the protonation of DEHiBA at the interface. Indeed, based on QM results in the gas phase and in PCM−water (Table S2), equilibria involving protonation of the amide from H_3O^+ at the interface cannot be precluded. O-protonation of the amide by H_3O^+ is also supported by a CPMD simulation we carried out on DMAA···H_3O^+ in a water cluster, showing that the proton rapidly transfers to form DMAAH$^+$ (Figure S21 in the Supporting Information). This protonated species is more surface active than neutral DEHiBA, as shown by MD simulations we performed on a mixture of these species contacted with acidic water: all protonated ligands sit at the interface (Figures S22 and S23 in the Supporting Information).

4. What Happens at the Interface upon Uranyl Extraction by Amide Ligands? The MD simulations on juxtaposed or randomly mixed liquids show that the aqueous and oil phases do not mix at the microscopic level and delineate interfaces onto which the free DEHiBA's and their complexes adsorb. The insolubility of uranyl nitrate in oil and of DEHiBA in water prevents complexation in either bulk phase, implying that the complexation process should occur right at the interface, i.e., in nanosized domains of the solution. In fact, uranyl nitrate is almost totally dissociated in water, but the proportion of $UO_2(NO_3)^+$ and $UO_2(NO_3)_2$ adducts increases with the nitric acid concentration,[64] and with the proximity to the interface (its lower dielectric constant and polarity, compared to the bulk water, yields a higher proportion of contact ion pairs). The neutral $UO_2(NO_3)_2$ species should approach more closely the interface than do the more hydrophilic $UO_2(NO_3)^+$ or UO_2^{2+} hydrated cations, facilitating an interfacial complexation process with DEHiBA's. As shown by the PMF and MD results, the $UO_2(NO_3)_2(DEHiBA)_2$ complexes are surface active. Accumulation of the complexes and of the free ligands at the interface reduces the interfacial tension and facilitates diffusion to the bulk oil phase, i.e., the extraction process. Furthermore, regarding the effect of nitric acid, one sees that the latter stabilizes the complex in the oil phase (by about 10 kcal/mol; Table S5), mainly via H-bonds between the $O_{(NO_3^-)}$ ligands and coextracted HNO_3 species (see, e.g., Figure S10), also explaining why the acid promotes the uranyl extraction.

In our demixing simulations of random mixtures of liquids, $UO_2(NO_3)_2$ and DEHiBA's different complexation results were obtained, depending on the electrostatic model. With both STD and POL models, no DEHiBA complexation occurs spontaneously, which might indicate that uranyl complexation energies calculated with AMBER are underestimated. Different comparisons with QM results (Table S3) indicate that this is not the case. With the three tested models, DEHiBA should displace water from $UO_2(NO_3)_2(H_2O)_2$ to afford the $UO_2(NO_3)_2(DEHiBA)_2$ complex: the resulting energy gain amounts to 6, 15, and 37 kcal/mol, respectively, with the STD, POL, and SCAL models. Note that the POL value is in the order of magnitude of the QM value of 10.1 kcal/mol, obtained with the DMAA mimics of DEHiBA. Thus, the lack of spontaneous formation of $UO_2(NO_3)_2(DEHiBA)_2$ complexes with the STD and POL models is more likely due to the corresponding kinetic barriers that involve, among others, water stripping from the uranyl nitrate complex. Not surprisingly, when DEHiBA is depicted with the scaled charges that exaggerate its complexation energy, it complexes uranyl nitrate during the demixing dynamics.

Regarding the U^{VI}/Ln^{3+} extraction selectivity displayed by amide ligands (and TBP), we do not find marked difference between the interfacial behavior of the corresponding $UO_2(NO_3)_2(DEHiBA)_2$ and $Eu(NO_3)_3(DEHiBA)_3$ complexes,

dx.doi.org/10.1021/jp4028386 | J. Phys. Chem. B XXXX, XXX, XXX−XXX

suggesting that the lack of Ln^{3+} extraction more likely stems for lower stability constants of their complexes, rather than from different partitioning between the two phases, once the complexes are formed.

5. Comparison of DEHiBA with TBP. The present study points to several analogies between DEHiBA and TBP as extracting agents, when simulated in similar conditions. Both are surface active, but DEHiBA is more hydrophobic and less surface active than TBP, as judged from their free energy profiles for interface crossing (compare Figure 3 for DEHiBA and Figure 6 of ref 25 for TBP). Likewise, the $UO_2(NO_3)_2(DEHiBA)_2$ complex is more hydrophobic and less surface active than the $UO_2(NO_3)_2(TBP)_2$ analogue (compare Figure 4 for DEHiBA and Figure 9 of ref 25 for TBP). When simulated by MD in similar conditions, both types of complexes adsorb at water/oil interfaces (where, for TBP, oil = chloroform,[46] $SC-CO_2$,[24,32] hexane,[25] or dodecane[65]). We note that these simulations represented uranyl nitrate with integer charges (q_{UO_2} = 2.0 e and q_{NO_3} = −1.0 e), rendering it more hydrophilic than with, for instance, ESP charges. Indeed, using adapted ESP charges (q_{UO_2} = 1.263 e and q_{NO_3} = −0.632 e), Ye et al. found that the TBP complex diffuses from the interface to the oil phase during the dynamics, indicating that it is weakly, or even not, surface active.[66] Comparison of surface activities of the TBP and DEHiBA complexes thus deserves further investigations as a function of their electrostatic representation (for a recent related study, see, e.g., the case of interface crossing by druglike molecules[67]).

In demixing simulations of water/oil mixtures containing the free ligands and uranyl nitrate, DEHiBA and TBP behave differently, since DEHiBA simulated with STD or POL models does not complex uranyl nitrate, whereas TBP spontaneously formed $UO_2(NO_3)_2(TBP)_1(H_2O)_1$ or $UO_2(NO_3)_2(TBP)_2$ adducts that adsorbed at the interface,[24,68] as supported by PMF results.[25] In our simulations, such complexes form with DEHiBA only when its ESP charges are scaled by 1.5, thereby exaggerating its affinity for uranyl nitrate. On the other hand, comparing the AMBER results for the TBP versus DEHiBA complexation by $UO_2(NO_3)_2$ (using TBP charges from ref 46) yields a (too high; see below) preference for TBP by 36.7 kcal/mol with the STD model, and 13.9 kcal/mol with the POL model. When the SCAL model is used for DEHiBA, the preference for TBP reduces to 4.5 kcal/mol, explaining why DEHiBA behaves more like TBP with this model.

Further insights into the affinity of $UO_2(NO_3)_2$ for amides versus TBP ligands can be obtained by QM calculations, using either DMAA or DMtBA (see Scheme 1) and TMP (trimethyl phosphate) as mimics, for simplicity. The results (Table S4) indicate that amides and TMP are stronger ligands than water (by about 10 kcal/mol in the gas phase and in PCM−water), a requisite to form the hydrophobic complex. Furthermore, the calculated preference over water amounts to 10.1 kcal/mol for DMAA, 8.3 kcal/mol for DMtBA, and 9.3 kcal/mol for TMP, indicating that the three types of ligands have comparable affinities for $UO_2(NO_3)_2$. A recent QM study of $UO_2(NO_3)_2$ complexes with alkyl-substituted amides[12] has shown that, depending on the ligand softness and polarizability, complexation energies can vary by up to 10 kcal/mol, suggesting that DEHiBA (not considered in ref 12) should interact better then DMAA, and thus better than TBP with $UO_2(NO_3)_2$.

CONCLUSION

To summarize, we present nanoscopic views of interfacial features of an important extraction system, a "green" alternative over TBP for uranyl separation by liquid−liquid extraction. Because the systems are inherently heterogeneous and complex and involve many competing interactions (nitric acid/ligands/uranyl/counterions, water/oil), the results cannot pretend to be quantitative. Model dependence is highlighted by a comparison of three typical electrostatic representations, one of which including atomic polarizabilities. With the latter, more suitable to depict aqueous interfaces, oil-soluble complexes (and, presumably, hydrophobic surface-active species) have a lower affinity for the interface than without polarization. Overall, the results point to the key role and characteristics of the interface in the complexation and extraction processes, calling for further investigations. On the computational side, as reported for other uranyl complexes,[69,70] MD and PMF calculations based on quantum mechanical (for instance DFT) representation of the potential energy of the whole system should give more quantitative insights into the detailed complexation process of DEHiBA in solution and, ultimately, at the interface. The state of nitric acid in the presence of interfacial ligands (like amides, TBP) also deserves further theoretical and spectroscopic investigations.[71] The resulting views combined with the time evolution of the spectroscopic signature[21] will afford deeper insights in the interface crossing, a process of utmost importance in fields like separation by liquid−liquid extraction, interfacial nanochemistry,[72] electrochemistry,[73] biphasic catalysis, drug delivery, or biological processes.[74] Beyond the interface, another important facet of assisted ion extraction involves the supramolecular organization of the organic phase, possibly involving aggregates of ligands and their complexes, higher-sized heterogeneities like micelles or microemulsions, or third phase formation in acidic conditions.[75,76]

ASSOCIATED CONTENT

Supporting Information

Tables S1−S12 with atomic charges and polarizabilities, tests on QM versus AMBER interaction energies, energy components analysis, solvation features of O(DEHiBA), HNO_3 and H_3O^+, surface tensions and diffusion coefficients. Figures S1−S23 include snapshots of all simulated biphasic systems, density curves, water surface, snapshots along the PMF trajectories, PMF results for HNO_3 across the interface, and CPMD results for proton transfer to DMMA. This material is available free of charge via the Internet at http://pubs.acs.org.

AUTHOR INFORMATION

Corresponding Author

*E-mail: wipff@unistra.fr.

Notes

The authors declare no competing financial interest.

ACKNOWLEDGMENTS

The authors are grateful to IDRIS, CINES, and Université de Strasbourg for computer resources, and to Etienne Engler,

Alain Chaumont, and Rachel Schurhammer for assistance and discussions. Support from the ANR ILLA is also acknowledged.

REFERENCES

(1) Musikas, C.; Schulz, W. W. Solvent Extraction in Nuclear Science and Technology. In *Principles and Practices of Solvent Extraction*; Rydberg, J., Musikas, C., Choppin, G. R., Eds.; M. Dekker, Inc.: New York, 1992; Vol. *11*, pp 413−447.

(2) Cecille, L.; Casarci, M.; Pietrelli, L. *New Separation Chemistry Techniques for Radioactive Waste and Other Specific Applications*; Elsevier Applied Science: London, 1991; pp 307.

(3) Mathur, J. N.; Murali, M. S.; Nash, K. L. Actinide Partitioning - A Review. *Solvent Extr. Ion Exch.* **2001**, *19*, 357−390.

(4) Madic, C.; Lecomte, M.; Baron, P.; Boullis, B. Separation of Long-Lived Radionuclides from High Active Nuclear Waste. *C.R. Phys.* **2002**, *3*, 797−811.

(5) Siddal, T. H. I. Effects of Structure of N,N-disubstituted Amides on their Extraction of Actinide and Zirconium Nitrates and of Nitric Acid. *J. Phys. Chem.* **1960**, *64*, 1863−1866.

(6) Musikas, C. Potentiality of Nonorganophosphorus Extractants in Chemical Separations of Actinides. *Sep. Sci. Technol.* **1988**, *23*, 1211−1226.

(7) Musikas, C.; Condamines, N.; Cuillerdier, C. Separation Chemistry for the Nuclear Industry. *Anal. Sci. Suppl.* **1991**, *7*, 11−16.

(8) Gasparini, G. M.; Grossi, G. Long Chain Disubstituted Aliphatic Amides as Extracting Agents in Industrial Applications of Solvent Extraction. *Solvent Extr. Ion Exch.* **1986**, *4*, 1233−1271.

(9) Ban, Y.; Hotuku, S.; Morita, Y. Distribution of $U^{(VI)}$ and $Pu^{(IV)}$ by N,N-di(2-ethylhexyl)Butanamide in Continuous Counter-Current Extraction with Mixer-Settler Extractor. *Solvent Extr. Ion Exch.* **2012**, *30*, 142−155.

(10) Condamines, N.; Musikas, C. The Extraction by N,N-dialkylamides. II. Extraction of Actinide Cations. *Solvent Extr. Ion Exch.* **1992**, *10*, 69−100.

(11) Rabbe, C.; Madic, C.; Godard, A. Molecular Modeling Study of Uranyl Nitrate Extraction with Monoamides I. Quantum Chemistry Approach. *Solvent Extr. Ion Exch.* **1998**, *16*, 1091−1109.

(12) Prestianni, A.; Joubert, L.; Chagnes, A.; Cote, G.; Adamo, C. A Density Functional Theory Study of Uranium(VI) Nitrate Monoamide Complexes. *Phys. Chem. Chem. Phys.* **2011**, *13*, 19371−19377.

(13) Varnek, A.; Fourches, D. Successful "In Silico" Design of New Efficient Uranyl Binders. *Solvent Extr. Ion Exch.* **2007**, *25*, 433−462.

(14) Miguirditchian, M.; Sorel, C.; Cames, B.; Bisel, I.; Baron, P.; Espinoux, D.; Calor, J.-N.; Viallesoubranne, C.; Lorrain, B.; Masson, M. *Global 2009*; Paris, France, 2009; pp 1032−1035.

(15) Pathak, P. N.; Prabhu, D. R.; Ruikar, P. B.; Mancha, V. K. Evaluation of Di(2-Ethylhexy)Isobutyramide (D2EHiBA) as a Process Extractant for the Recovery of ^{233}U from Irradiated Th. *Solvent Extr. Ion Exch.* **2002**, *20*, 293−311.

(16) Danesi, P. R.; Chiarizia, R.; Coleman, C. F. The Kinetics of Metal Solvent Extraction. In *Critical Reviews in Analytical Chemistry*; Campbell, B., Ed.; CRC Press: Boca Raton, FL, 1980; Vol. *10*, p 1.

(17) Watarai, H. What's Happening at the Liquid-Liquid Interface in Solvent Extraction Chemistry? *Trends Anal. Chem.* **1993**, *12*, 313−318.

(18) Stevens, G. W.; Perera, J. M.; Grieser, F. Interfacial Aspects of Metal Ion Extraction in Liquid-Liquid Systems. *Rev. Chem. Eng.* **2001**, *17*, 87−110.

(19) Szymanowski, J. Kinetics and Interfacial Phenomena. *Solvent Extr. Ion Exch.* **2000**, *18*, 729−751.

(20) Martin-Gassin, G.; Gassin, P. M.; Couston, L.; Diat, O.; Benichou, E.; Brevet, P. F. Second Harmonic Generation Monitoring of Nitric Acid Extraction by a Monoamide at the Water−Dodecane Interface. *Phys. Chem. Chem. Phys.* **2011**, *13*, 19580−19586.

(21) Martin-Gassin, G.; Gassin, P. M.; Couston, L.; Diat, O.; Benichouc, E.; Brevet, P. F. Nitric acid Extraction with Monoamide and Diamide Monitored by Second Harmonic Generation at the Water/Dodecane Interface. *Colloids Surf., A* **2012**, *413*, 130−135.

(22) Nave, S.; Mandin, C.; Martinet, L.; Berthon, L.; Testard, F.; Madic, C.; Zemb, T. Supramolecular Organisation of Tri-*n*-butyl Phosphate in Organic Diluent on Approaching Third Phase Transition. *Phys. Chem. Chem. Phys.* **2004**, *6*, 799−808.

(23) Meridiano, Y.; Berthon, L.; Crozes, X.; Sorel, C.; Dannus, P.; Antonio, M. R.; Chiarizia, R.; Zemb, T. Aggregation in Organic Solutions of Malonamides: Consequences for Water Extraction. *Solvent Extr. Ion Exch.* **2009**, *27*, 607−637.

(24) Baaden, M.; Schurhammer, R.; Wipff, G. Molecular Dynamics Study of the Uranyl Extraction by Tri-*n*-butylphosphate (TBP): Demixing of Water/"Oil"/TBP Solutions with a Comparison of Supercritical CO_2 and Chloroform. *J. Phys. Chem. B* **2002**, *106*, 434−441.

(25) Jayasinghe, M.; Beck, T. L. Molecular Dynamics Simulations of the Structure and Thermodynamics of Carrier-Assisted Uranyl Ion Extraction. *J. Phys. Chem. B* **2009**, *113*, 11662−11671.

(26) Cui, S.; de Almeida, V. F.; Hay, B. P.; Ye, X.; Khomami, B. Molecular Dynamics Simulation of Tri-n-butyl-Phosphate Liquid: A Force Field Comparative Study. *J. Phys. Chem. B* **2012**, *16*, 305−313.

(27) Troxler, L.; Wipff, G. Interfacial Behaviour of Ionophoric Systems: Molecular Dynamics Studies on 18-crown-6 and its Complexes at the Water - Chloroform Interface. *Anal. Sci.* **1998**, *14*, 43−56.

(28) Baaden, M.; Berny, F.; Muzet, N.; Troxler, L.; Wipff, G. Interfacial Features of Assisted Liquid-Liquid Extraction of Uranyl and Cesium Salts: a Molecular Dynamics Investigation. In *Calixarenes for Separation*; Lumetta, G., Rogers, R., Gopalan, A., Eds.; ACS Symposium Series 757; American Chemical Society: Washington, DC, 2000; pp 71−85.

(29) Sieffert, N.; Wipff, G. Alkali Cation Extraction by a Calix[4]crown6 to Room Temperature Ionic Liquids. The Effect of Solvent Anion and Humidity Investigated by Molecular Dynamics Simulations. *J. Phys. Chem. A* **2006**, *110*, 1106−1117.

(30) Jost, P.; Galand, N.; Schurhammer, R.; Wipff, G. 222 Cryptand and its Cryptates at the Water/Chloroform Interface: Molecular Dynamics Simulations of Concentrated Solutions. *Phys. Chem. Chem. Phys.* **2002**, *4*, 335−344.

(31) Pathak, P. N.; Veeraraghavan, R.; Prabhu, D. R.; Mahajan, G. R.; Manchanda, V. K. Separation Studies of Uranium and Thorium Using di-2-Ethylhexyl Isobutyramide (D2EHiBA). *Sep. Sci. Technol.* **1999**, *34*, 2601−2614.

(32) Schurhammer, R.; Wipff, G. Uranyl Extraction by TBP from a Nitric Aqueous Solution to SC-CO_2: MD Simulations of Phase Demixing and Interfacial Systems. In *Separations and Processes Using Supercritical Carbon Dioxide*; Gopalan, A. S., Wai, C., Jacobs, H., Eds.; American Chemical Society: Washington, DC, 2003; Vol. *860*, Chapter 15, pp 223−244.

(33) Case, D. A.; Darden, T. A.; Cheatham III, T. E.; Simmerling, C. L.; Wang, J.; Duke, R. E.; Luo, R.; Crowley, M.; Walker, R. C.; Zhang, W. et al. *AMBER10*; University of California: San Francisco, 2008.

(34) Jorgensen, W. L.; Chandrasekhar, J.; Madura, J. D.; Impey, R. W.; Klein, M. L. Comparison of Simple Potential Functions for Simulating Liquid Water. *J. Chem. Phys.* **1983**, *79*, 926−936.

(35) Jorgensen, W. L.; Tirado-Rives, J. The OPLS Potential Functions for Proteins. Energy Minimizations for Crystals of Cyclic Peptides and Crambin. *J. Am. Chem. Soc.* **1988**, *110*, 1657−1666.

(36) Guilbaud, P.; Wipff, G. Force Field Representation of the UO_2^{2+} Cation from Free Energy MD Simulations in Water.Tests on its 18-crown-6 and NO_3^- Adducts, and on its Calix[6]arene^{6-} and CMPO Complexes. *J. Mol. Struct. THEOCHEM* **1996**, *366*, 55−63.

(37) Rai, N.; Tiwari, S.; Maginn, E. Force Field Development for Actinyl Ions via Quantum Mechanical Calculations: An Approach to Account for Many Body Solvation Effects. *J. Phys. Chem. B* **2012**, *116*, 10885−10897.

(38) Dang, L. X.; Rice, J. E.; Caldwell, J.; Kollman, P. A. Ion Solvation in Polarizable Water: Molecular Dynamics Simulations. *J. Am. Chem. Soc.* **1991**, *113*, 2481−2486.
(39) Caldwell, J. W.; Kollman, P. A. Structure and Properties of Neat Liquids Using Nonadditive Molecular Dynamics: Water, Methanol, and *N*-Methylacetamide. *J. Phys. Chem.* **1995**, *99*, 6208−6219.
(40) York, D. M.; Darden, T. A.; Pedersen, L. G. The Effect of Long-Range Electrostatic Interactions in Simulations of Macromolecular Crystals: A Comparison of the Ewald and Truncated List Methods. *J. Chem. Phys.* **1993**, *99*, 8345−8348.
(41) Berendsen, H. J. C.; Postma, J. P. M.; van Gunsteren, W. F.; DiNola, A. Molecular Dynamics with Coupling to an External Bath. *J. Chem. Phys.* **1984**, *81*, 3684−3690.
(42) Kollman, P. Free Energy Calculations: Applications to Chemical and Biochemical Phenomena. *Chem. Rev.* **1993**, *93*, 2395−2417.
(43) Frisch, M. J.; Trucks, G. W.; Schlegel, H. B.; Scuseria, G. E.; Robb, M. A.; Cheeseman, J. R.; Scalmani, G.; Barone, V.; Mennucci, B.; Petersson, G. A. et al. *Gaussian 09 Revision B.01*; Gaussian, Inc.: Wallingford, CT, 2010.
(44) Institut für Theoretische Chemie, Universität Stuttgart. ECPs and corresponding valence basis sets. http://www.theochem.uni-stutgart.de.
(45) Tomasi, J.; Mennucci, B.; Cammi, R. Quantum Mechanical Continuum Solvation Models. *Chem. Rev.* **2005**, *105*, 2999−3093.
(46) Baaden, M.; Burgard, M.; Wipff, G. TBP at the Water - Oil Interface: the Effect of TBP Concentration and Water Acidity Investigated by Molecular Dynamics Simulations. *J. Phys. Chem. B* **2001**, *105*, 11131−11141.
(47) Vacha, R.; Horinek, D.; Berkowitz, M. L.; Jungwirth, P. Hydronium and Hydroxide at the Interface between Water and Hydrophobic Media. *Phys. Chem. Chem. Phys.* **2008**, *10*, 4975−4980.
(48) Jungwirth, P.; Winter, B. Ions at Aqueous Interfaces: From Water Surface to Hydrated Proteins. *Annu. Rev. Phys. Chem.* **2008**, *59*, 343−366.
(49) Chang, T. M.; Dang, L. X. Molecular Dynamics Simulations of CCl_4-H_20 Liquid-Liquid Interface with Polarizable Potential Models. *J. Chem. Phys.* **1995**, *104*, 6772−6783.
(50) Benjamin, I. Molecular Structure and Dynamics at Liquid-Liquid Interfaces. *Annu. Rev. Phys. Chem.* **1997**, *48*, 407−451.
(51) Schurhammer, R.; Wipff, G. Effect of the TBP and Water on the Complexation of Uranyl Nitrate and the Dissolution of Nitric Acid into Supercritical CO_2 . A Theoretical Study. *J. Phys. Chem. A* **2005**, *109*, 5208−5216.
(52) Dang, L. X.; Chang, T.-M. Molecular Mechanism of Ion Binding to the Liquid/Vapor Interface of Water. *J. Phys. Chem. B* **2002**, *106*, 235−238.
(53) Chang, T.-M.; Dang, L. X. Recent Advances in Molecular Simulations of Ion Solvation at Liquid Interfaces. *Chem. Rev.* **2005**, *106*, 1305−1322.
(54) Mucha, M.; Frigato, T.; Levering, L. M.; Allen, H. C.; Tobias, D. J.; Dang, L. X.; Jungwirth, P. Unified Molecular Picture of the Surface of Aqueous Acid, Base, and Salt Solutions. *J. Phys. Chem. B* **2005**, *109*, 7617−7623.
(55) Jungwirth, P.; Tobias, D. J. Specific Ion Effects at the Air/Water Interface. *Chem. Rev.* **2006**, *106*, 1259−1281.
(56) Cummings, O. T.; Wick, C. D. Computational Study of Cation Influence on Anion Propensity for the Air−Water Interface. *Chem. Phys. Lett.* **2010**, *500*, 41−45.
(57) Yagasaki, T.; Saito, S.; Ohmine, I. Effects of Nonadditive Interactions on Ion Solvation at the Water/Vapor Interface: A Molecular Dynamics Study. *J. Phys. Chem. A* **2010**, *114*, 12573−12584.
(58) Pluhařová, E.; Mason, P. E.; Jungwirth, P. Ion Pairing in Aqueous Lithium Salt Solutions with Monovalent and Divalent Counter-Anions. *J. Phys. Chem. A* **2013**, DOI: 10.1021/jp402532e.
(59) Walker, D. S.; Richmond, G. L. Depth Profiling of Water Molecules at the Liquid-Liquid Interface Using a Combined Surface Vibrational Spectroscopy and Molecular Dynamics Approach. *J. Am. Chem. Soc.* **2007**, *129*, 9446−9451.
(60) Scatena, L. F.; Richmond, G. L. Orientation, Hydrogen Bonding, and Penetration of Water at the Organic/Water Interface. *J. Phys. Chem. B* **2001**, *105*, 11240−11250.
(61) Pathak, P. N.; Kumbhare, L. B.; Manchanda, V. K. Effect of Structure of N,N-dialkyl Amides on the Extraction of $U^{(VI)}$ and $Th^{(VI)}$: a Thermodynamic Study. *Radiochim. Acta* **2001**, *89*, 447−452.
(62) Lewis, T.; Winter, B.; Stern, A. C.; Bae, M. D.; Mundy, C. J.; Tobias, D. J.; Hemminger, J. C. Dissociation of Strong Acid Revisited: X-ray Photoelectron Spectroscopy and Molecular Dynamics Simulations of HNO3 in Water. *J. Phys. Chem. B* **2011**, *115*, 9445−9451.
(63) Shamay, E. S.; Buch, V.; Parrinello, M.; Richmond, G. L. At the Water's Edge: Nitric Acid as a Weak Acid. *J. Am. Chem. Soc.* **2007**, *129*, 12910−12911.
(64) Ye, X.; Smith, R. B.; Cui, S.; deAlmeida, V.; Khomami, B. Influence of Nitric Acid on Uranyl Nitrate Association in Aqueous Solutions: A Molecular Dynamics Simulation Study. *Solvent Extr. Ion Exch.* **2010**, *28*, 1−18.
(65) Ye, X.; Cui, S.; de Almeida, V.; Khomami, B. Interfacial Complex Formation in Uranyl Extraction by Tributyl Phosphate in Dodecane Diluent: a Molecular Dynamics Study. *J Phys. Chem. B.* **2009**, *113*, 9852−9862.
(66) Ye, X.; Cui, S.; deAlmeida, V. F.; Hay, B. P.; Khomami, B. Uranyl Nitrate Complex Extraction into TBP/Dodecane Organic Solutions: a Molecular Dynamics Study. *Phys. Chem. Chem. Phys.* **2010**, *12*, 15406−15409.
(67) Paloncyova, M.; Berka, K.; Otyepka, M. Convergence of Free Energy Profile of Coumarin in Lipid Bilayer. *J. Chem. Theory Comput.* **2012**, *8*, 1200−1211.
(68) Baaden, M.; Berny, F.; Muzet, N.; Schurhammer, R.; Troxler, L.; Wipff, G. Separation of Cs^+ and UO_2^{2+} Cations by Liquid-Liquid Extraction: Computer Simulations of the Demixing of Water/Oil Binary Solutions. In *Euradwaste 1999: Radioactive Waste Management Strategies and Issues*; Davies, C., Ed.; European Commission: Brussels, 2000; Vol. EUR 19143 EN, pp 519−522.
(69) Bühl, M.; Sieffert, N.; Chaumont, A.; Wipff, G. Water versus Acetonitrile Coordination to Uranyl. Effect of Chloride Ligands. *Inorg. Chem.* **2012**, *51*, 1943−1952.
(70) Bühl, M.; Wipff, G. Insights into Uranyl Chemistry from Molecular Dynamics Simulations. *ChemPhysChem* **2011**, *12*, 3095−3105.
(71) Soule, M. C. K.; Blower, P. G.; Richmond, G. L. Nonlinear Vibrational Spectroscopic Studies of the Adsorption and Speciation of Nitric Acid at the Vapor/Acid Solution Interface. *J. Phys. Chem. A* **2007**, *111*, 3349−3357.
(72) Watarai, H.; Teramae, N.; Sawada, T. *Interfacial Nanochemistry. Molecular Science and Engineering at Liquid-Liquid Interfaces*; Kluwer Academic Plenum: New York, 2005; pp 321.
(73) Girault, H. H.; Schiffrin, D. J. Electrochemistry of Liquid-Liquid Interfaces. In *Electroanalytical Chemistry*; Bard, A. J., Ed.; Dekker: New York, 1989; Vol. *15*, pp 1−141.
(74) Volkov, A. G.; Brevet, P. F. Liquid Interfaces in Chemical, Biological and Pharmaceutical Applications. In *Nonlinear Optics at Liquid/Liquid Interfaces*; M. Dekker: New York, 2001; p 551.
(75) Osseo-Asare, K. Aggregation, Reversed Micelles, and Microemulsions in Liquid-Liquid Extraction: the Tri-n-Butyl Phosphate-Diluent-Water-Electrolyte System. *Adv. Colloid Interface Sci.* **1991**, *37*, 123−173.
(76) Bauer, C.; Bauduin, P.; Dufrêche, J. F.; Zemb, T.; Diat, O. Liquid/liquid Metal Extraction: Phase Diagram Topology Resulting from Molecular Interactions between Extractant, Ion, Oil and Water. *Eur. Phys. J. Spec. Top.* **2012**, *213*, 225−241.